





# Ginger Extract–Loaded Transethosomes for Effective Transdermal Permeation and Anti-Inflammation in Rat Model

Abeer S Hassan <sup>1</sup>, Amal Hofni <sup>2</sup>, Mohammed AS Abourehab <sup>3</sup>, Iman AM Abdel-Rahman <sup>4</sup>

<sup>1</sup>Department of Pharmaceutics, Faculty of Pharmacy, South Valley University, Qena, Egypt; <sup>2</sup>Department of Pharmacology and Toxicology, Faculty of Pharmacy, South Valley University, Qena, Egypt; <sup>3</sup>Department of Pharmaceutics and Industrial Pharmacy, College of Pharmacy, Minia University, Minia, Egypt; <sup>4</sup>Department of Pharmacognosy, Faculty of Pharmacy, South Valley University, Qena, Egypt

Correspondence: Abeer S Hassan, Department of Pharmaceutics, Faculty of Pharmacy, South Valley University, Qena, Egypt, Tel +201012060262, Email [abeer.saad@svu.edu.eg](mailto:abeer.saad@svu.edu.eg)

**Introduction:** Ginger extract (GE) has sparked great interest due to its numerous biological benefits. However, it suffers from limited skin permeability, which challenges its transdermal application. The target of the current work was to develop transethosomes as a potential nanovehicle to achieve enhanced transdermal delivery of GE through the skin.

**Methods:** GE-loaded transethosomes were prepared by cold injection using different edge activators. The fabricated nanovesicles were evaluated for particle size,  $\zeta$ -potential, encapsulation efficiency, and in vitro drug release. The selected formulation was then laden into the hydrogel system and evaluated for ex vivo permeability and in vivo anti-inflammatory activity in a carrageenan-induced rat-paw edema model.

**Results:** The selected formulation comprised of sodium deoxycholate exhibited particle size of  $188.3 \pm 7.66$  nm,  $\zeta$ -potential of  $-38.6 \pm 0.08$  mV, and encapsulation efficiency of  $91.0\% \pm 0.24\%$ . The developed transethosomal hydrogel containing hydroxypropyl methylcellulose was homogeneous, pseudoplastic, and demonstrated sustained drug release. Furthermore, it exhibited improved flux ( $12.61 \pm 0.45$   $\mu\text{g}\cdot\text{cm}^2/\text{second}$ ), apparent skin permeability ( $2.43 \pm 0.008 \times 10^{-6}$  cm/second), and skin deposition compared to free GE hydrogel. In vivo testing and histopathological examination revealed that the GE transethosomal hydrogel exhibited significant inhibition of edema swelling compared to free GE hydrogel and ketoprofen gel. The animals that were treated with ginger transethosome hydrogel showed a significant decrement in reactive oxygen species and prostaglandin  $E_2$  compared to untreated animals.

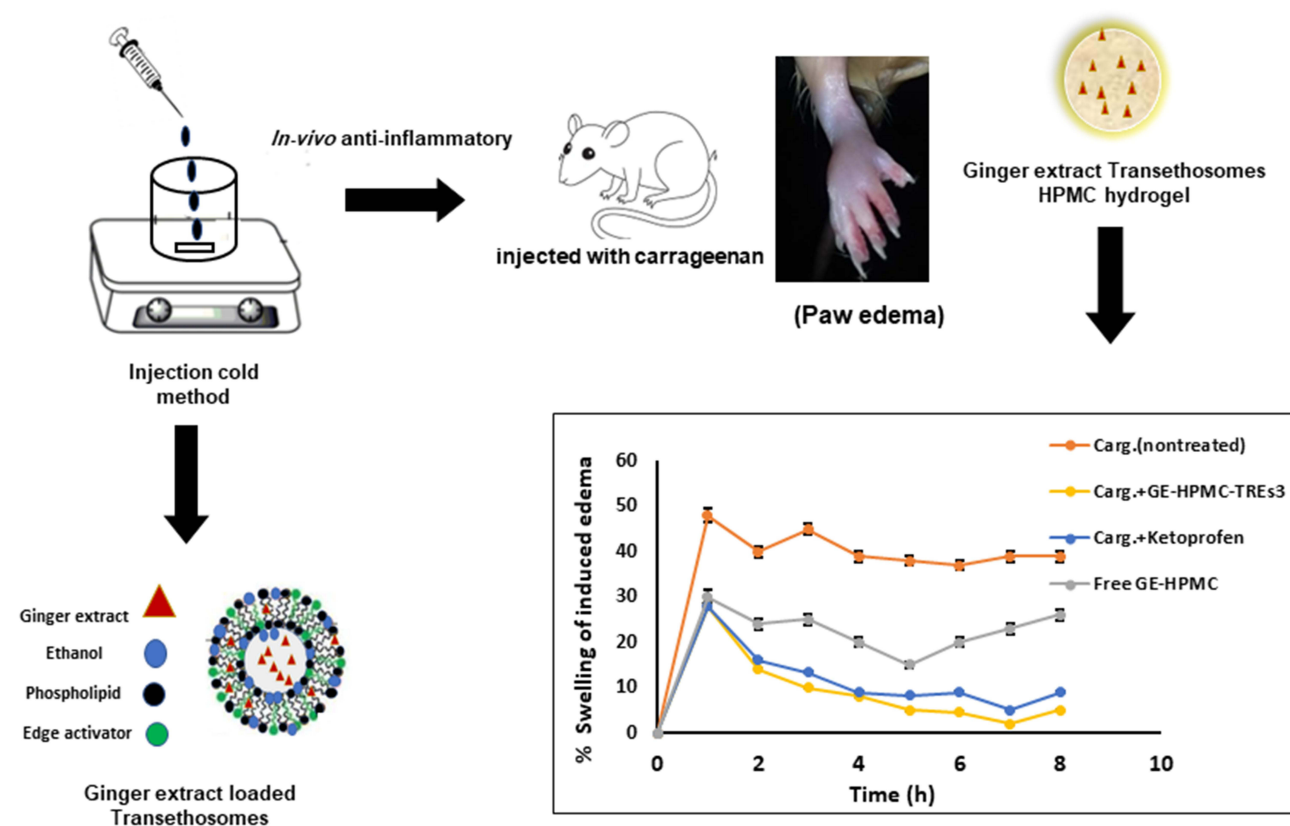
**Conclusion:** Transethosomes might be a promising new vehicle for GE for effective skin permeation and anti-inflammation. To the best of our knowledge, this work is the first utilization of transethosomes laden into hydrogel as a novel transdermal delivery system of GE.

**Keywords:** nanovesicles, transethosomes, ginger, ex vivo permeation, transdermal delivery, inflammation

## Introduction

Several pathological disorders, such as rheumatoid arthritis and osteoarthritis, are triggered by inflammation. Active drug products that inhibit inflammation are potentially used to prevent the development of these disorders. Though different anti-inflammatory agents, either steroidal anti-inflammatory drugs (SAIDs) or non-SAIDs (NSAIDs), are utilized for inflammation management, they show several adverse effects. Using SAIDs may cause obesity and sodium retention, which result in serious health hazardous, including liver toxicity and gastrointestinal ulcers, the most common NSAID side effects.<sup>1</sup> Clinical investigations have found local adverse effects in 6.3% of participants following local administration of NSAIDs, such as irritation at the application site and itching. Several studies have reported on new drug products that improve the anti-inflammatory performance of drugs and limit their undesirable effects. Natural plants are characterized by several bioactive phytochemicals possessing anti-inflammatory activity.<sup>2</sup> Employing natural medicinal plants may have some advantages compared to conventional pharmaceuticals, such as a better safety profile and lower price. However, limited bioavailability, tissue permeability, and low levels of phenolic moieties in plant extracts are the

## Graphical Abstract



major challenges of using these medicinal plant products.<sup>3</sup> These shortcomings necessitate the production of reliable delivery nanovehicles to improve their permeability and boost therapeutic performance.

Transdermal delivery systems using nanocarriers can offer sufficient quantities of active ingredients for long periods and avoid their extensive liver metabolism.<sup>4</sup> Moreover, transdermal delivery of nanocarriers can be used to enhance local dermal effects and permeation through the skin for systemic performance.<sup>5</sup> Recently, vesicular nanocarriers have received great interest in applications of topical and transdermal drug delivery because of their similarity to cell-membrane structure. They consist of an aquatic core surrounded by a lipid bilayer, which allows them to encapsulate both hydrophilic and hydrophobic drug molecules.<sup>6</sup> Further, these nanovesicles provide sustained drug release and deep penetration of the skin layers.<sup>7</sup>

Liposomes are among the most frequently investigated lipid nanovesicles. These nanovesicles are spherical and made of phospholipid bilayers surrounding aqueous cores.<sup>8,9</sup> The limited physical and chemical stability of liposomes hinders their pharmaceutical application. New deformable nanovesicles have been designed, such as ethosomes, transfersomes, and transethosome (TREs), to enhance the stability of conventional liposomes. A new category of vesicular structures, composed of phospholipid, ethanol (20%–40%), and water, are termed “ethosomes.” Using ethosomes enables additional advantages, including improved skin permeation of the drug through the stratum corneum and subsequent retention in the skin layers.<sup>10</sup> A novel type of nanovesicles, TREs have been studied in recent literature. They are elastic, stable, malleable, biodegradable lipid nanovesicles combining the advantages of both ethosomes and transfersomes. Structurally, they are phospholipid carriers composed of basic components of ethosomes (lipid, ethanol, 20%–40%) and edge activators, such as Tween 80, sodium deoxycholate, and oleic acid.<sup>9,11</sup> TREs act via fluidizing and squeezing into tiny holes in the skin, resulting in improved skin penetration. The presence of ethanol and edge activators

allows them to stretch and pass through the skin without marked loss, thus offering efficient penetration of the vesicles.<sup>11,12</sup> Studies have reported that TREs exhibit efficient stabilizing effects and enhanced transdermal permeation of active natural products.<sup>5,13–15</sup>

One of the plants utilized traditionally for several inflammatory disorders is ginger (*Zingiber officinale*), which belongs to the family Zingiberaceae. It is widely used in medicinal purposes and dietary condiments due to its therapeutic and nutrition value.<sup>16</sup> Most traditional and complementary systems of medicine, such as Ayurveda, recommend ginger to manage various disease conditions as a result of their anti-inflammatory and antinausea properties.<sup>17,18</sup> In recent times, the rhizome, or root, of ginger has been widely studied for exhibiting antimicrobial, antitumor, antidiabetic, and antioxidant properties.<sup>19</sup> Fresh ginger has two wide-range categories: volatiles and nonvolatiles. Volatiles include sesquiterpene and monoterpene hydrocarbons, which are responsible for the distinct aroma and taste of ginger. Nonvolatile pungent compounds include gingerols, shogaols, paradols, and zingerone.<sup>16,20</sup>

Ginger extract (GE) has been known to exhibit anti-inflammatory activity by suppressing the biosynthesis of inflammatory mediators, 5-lipoxygenase and cyclooxygenase inhibition, and inhibition of nitric oxide production. These therapeutic activities may be attributed to the presence of different bioactive materials.<sup>17,21</sup> However, these bioactive materials have high molecular weight, limited solubility, poor bioavailability, and poor permeability across the skin that may affect the transdermal delivery of GE.<sup>4</sup> GE has been explored for its transdermal delivery using different nanocarrier systems. Bioadhesive dermal patches of ginger were developed by Rahman et al and utilized as an antibacterial agent.<sup>22</sup> They found that >80% of bacterial infections were inhibited after the application of ginger bioadhesive patches in an ex vivo *Staphylococcus aureus* infection model in rat skin. Priprem et al<sup>4</sup> encapsulated GE into niosome vesicles, then incorporated these into a gel for topical delivery. They found that GE niosomal gel enabled an improved anti-inflammatory effect in a croton oil-induced ear-edema mouse model. Abdallah et al<sup>23</sup> examined the anti-inflammatory activity of GE in carrageenan-induced paw edema in rats. They employed transdermal delivery of niosome vesicles laden into emulgel formulated with sesame oil, finding a remarkable effect of sesame oil on the improvement of anti-inflammatory performance of GE niosomes and revealing a synergistic effect of sesame oil with GE. In view of this, transdermal delivery of GE using prospective TRE vesicles can provide improved permeability of active ingredients in ginger that are responsible for anti-inflammatory activity.

The goal of the current study was to investigate the prospective effect of loading a novel nanocarrier, TRE vesicles with GE (GE-TREs), on enhanced skin permeability and performance in the management of inflammation. To the best of our knowledge, this is the first work to present the potential use of TRE hydrogel as a nanocarrier for GE transdermal delivery through the skin. GE-TREs were fabricated and characterized in terms of particle size,  $\zeta$ -potential, encapsulation efficiency (EE), and in vitro drug release. After that, the best GE-TRE formulation was incorporated into a hydrogel system using three gelling agents. The prepared ginger transethosomal hydrogels were evaluated in terms of viscosity, in vitro drug release, and ex vivo permeability through the skin of rats. Finally, the in vivo performance of the selected formulation was examined, employing carrageenan-induced paw edema in rats, and compared with free GE hydrogel and ketoprofen hydrogel as a reference anti-inflammatory.

## Materials and Methods

### Materials

Fresh ginger rhizome was purchased from a local market in Qena, Egypt. Identification of the plant was done at the Pharmacognosy Department, Faculty of Pharmacy, South Valley University, Qena, Egypt. A specimen (code Zo.82) was kept in the herbarium of the Pharmacognosy Department. Carrageenan, sodium deoxycholate, Tween 80, and cellulose membrane (molecular weight 12,000–14,000 Da cutoff) were obtained from Sigma Chemicals (St Louis, MO, USA). Phosphatidylcholine phospholipon 90G was purchased from Lipoid (Steinhausen, Switzerland). Cholesterol was obtained from Kanto Chemical (Tokyo, Japan). Sodium alginate was obtained from General Chemical and Pharmaceutical, Sudbury, UK. Chitosan (CS; low molecular weight, viscosity 100 cp, 98% degree of deacetylation) was obtained from Industrial Manufacturing, Tokyo, Japan. Hydroxypropyl methylcellulose 15,000 was obtained from El Gomhouria, Cairo, Egypt. Ethanol, potassium dihydrogen phosphate, and disodium hydrogen phosphate were purchased from the United

Company for Chemicals and Medical Preparations (Cairo, Egypt). All other chemicals and solvents were of analytical grade and used as received.

## Animal Studies

Adult male Sprague Dawley rats (weight 200–230 g, age 10–12 weeks) were utilized. The animals were obtained from the National Research Center, Giza, Egypt. During the experimental course, the animals were maintained under constant environmental conditions and subjected to cycling of dark and light of 14:10 h while food and water were available. They were left to adapt for 1 week, during which free access to standard commercial rat chow and tap water was offered. Blood samples were collected from the peripheral vein into sterile tubes at room temperature, and serum was collected and stored at  $-80^{\circ}\text{C}$  until use. Prostaglandin  $\text{E}_2$  ( $\text{PGE}_2$ ) and  $\text{TNF}\alpha$  concentrations were determined by ELISA.

## Preparation of Ginger Extract

Fresh rhizome was washed with deionized water, sliced, dried in the sun for 1 week, and dried again at  $50^{\circ}\text{C}$  in an oven for 6 h. The dried rhizome was divided into small pieces, powdered by an electronic mill, sieved, and stored in a well-closed dark glass container until being used.<sup>24</sup> The powdered plant material (300 g) was subjected to extraction by maceration in 1.5 L ethanol for 3 days with frequent stirring, followed by filtration. This process was repeated twice. The extract was then filtered using filter paper (Whatman 1) and evaporated utilizing a rotary evaporator under reduced pressure at  $40^{\circ}\text{C}$ . The solvent-free residue was stored at  $4^{\circ}\text{C}$  before use.<sup>25</sup>

## Spectrophotometric Analysis of Ginger Extract

GE (10 mg) was dissolved in ethanol and diluted to concentrations of 5, 10, 15, 20, 25, 30, 35, 40, 45, 50, and 100  $\mu\text{g}/\text{mL}$ . Then, the absorbance of these samples in the UV range of 200–600 was determined using a UV-vis spectrophotometer (Lisco, Bargteheide, Germany) using ethanol as a blank to measure the wavelength of maximum absorption ( $\lambda_{\text{max}}$ ) for GE.  $\lambda_{\text{max}}$  was found to be 285 nm, then the calibration curve was obtained.

## Preparation of Transethosomes Loaded with Ginger Extract

TRE nanovesicles were formulated utilizing cold injection using ethanol and distilled water at a ratio of 3:7 (v:v).<sup>13,26</sup> In brief, a mixture composed of GE, phospholipon 90G, and cholesterol was added to an edge activator (Span 80, Tween 80, and sodium deoxycholate) and dissolved in ethanol at  $30^{\circ}\text{C}$ . Afterward, the aqueous phase (distilled water) was added dropwise to the organic phase and stirred continuously at 2000 rpm for 30 min with a magnetic stirrer. The resultant TRE suspensions were vortexed for approximately 5 min, then sonicated for an additional 2 min at  $25^{\circ}\text{C}$ . The fabricated TRE preparations were left overnight at  $4^{\circ}\text{C}$  for further characterization. The composition of different TRE formulations is summarized in Table 1.

## In Vitro Characterization of Transethosomes Loaded with Ginger Extract

### Particle Size and $\zeta$ -Potential

The particle size and polydispersity index (PDI) of the GE-loaded TREs were determined at  $25^{\circ}\text{C}$  via dynamic laser light scattering (DLS) utilizing a Malvern Zetasizer Nanoseries ZS (Malvern Instruments, Worcestershire, UK) equipped with a backscattered light detector operating at  $173^{\circ}$ . The  $\zeta$ -potential of the fabricated TREs was measured via laser Doppler anemometry employing the Malvern Zetasizer. Determinations were conducted in triplicate.

### Drug-Encapsulation Efficiency and Drug-Loading Percentage

EE was calculated indirectly via measuring free untrapped content of GE employing UV-vis spectrophotometry. The untrapped drug was obtained using cooling centrifugation (benchtop refrigerated centrifuge, Centurion Scientific, Sussex, UK) at  $4^{\circ}\text{C}$  and 15,000 rpm for 1 h to separate it.<sup>27</sup> GE concentration in supernatant was estimated utilizing UV-vis spectrophotometry from a calibration curve of the hydroethanolic extract of ginger (wavelength at  $\lambda_{\text{max}}$  of 285 nm for maximum absorption). EE and drug loading (DL) were determined via equations (1) and (2).<sup>28</sup>

**Table I** Composition of ginger extract (GE) transethosome (TRE) nanovesicles per 10 mL colloidal dispersion, and composition of GE transethosomal and nontransethosomal hydrogel formulations

Transethosome formulations	GE (mg)	Phospholipid (mg)	Cholesterol (mg)	Span 80 (mg)	Tween 80 (mg)	Sodium deoxycholate (mg)	Ethanol (mL)	Water (mL)
TRE1	30	300	20	30	0	0	3	7
TRE2	30	300	20	0	30	0	3	7
TRE3	30	300	20	0	0	30	3	7
Hydrogel formulations	Content							
F1	GE-NaAlg (4% w:v)							
F2	GE-CS (2% w:v)							
F3	GE-HPMC (3% w:v)							
F4	GE-TRE3-NaAlg (4% w:v)							
F5	GE-TRE3-CS (2% w:v)							
F6	GE-TRE3-HPMC (3% w:v)							

**Note:** GE equivalent to 0.3% w:v in hydrogel formulations.

**Abbreviations:** CS, chitosan; HPMC, hydroxypropyl methylcellulose; GE-TRE3, GE-loaded TREs prepared using sodium deoxycholate; GE-TRE3-NaAlg (4%), NaAlg hydrogel containing GE-loaded TREs prepared using sodium deoxycholate; CS-TRE3, CS (2%) hydrogel containing GE-loaded TREs prepared using sodium deoxycholate; HPMC-TRE3, HPMC hydrogel (3%) GE-loaded TREs prepared using sodium deoxycholate.

$$EE\% = \frac{\text{Total extract content} - \text{Free extract content}}{\text{total extract content}} \times 100 \quad (1)$$

$$DL\% = \frac{\text{Total extratract content in vesicles}}{\text{Total weight of tested vesicles}} \times 100 \quad (2)$$

### Transmission Electron Microscopy

TEM (100 CX II; JEOL, Tokyo, Japan) was used for imaging of the TRE vesicles. Transethosomal dispersion (selected formulation) was diluted tenfold utilizing distilled water, then a drop was placed on a copper grid with a 300-mesh carbon coating and allowed to sit for a minute to allow some of the vesicles to stick to the carbon substrate. A piece of filter paper was used to remove extra dispersion, and the grid was then rinsed twice in deionized water for 3–5 seconds. The sample was then examined under a microscope utilizing 10–100× magnification and an accelerating voltage of 100 kV.

### Fourier-Transform Infrared Spectroscopy Analysis

The FT-IR spectra of free GE, blank empty TREs, and GE TREs (GE-TREs) were detected employing a Nicolet 6700 FT-IR spectrometer (Thermo Fisher Scientific, Waltham, MA, USA). The examined preparations were blended with spectroscopic-grade potassium bromide (KBr), then crushed into disks using a hydraulic press (15,000 lb). The scanning range for the samples was 4000–400  $\text{cm}^{-1}$ .

### Stability of Transethosomes Loaded with Ginger Extract

GE TREs were kept in a sealed 20 mL glass vial and investigated for 1 month at  $4^\circ \pm 1^\circ \text{C}$  and  $5^\circ \pm 1^\circ \text{C}$ .<sup>29</sup> Physical stability of the TRE dispersion was evaluated based on visual inspection of sedimentation and particle-size measurement. TREs were tested for EE after 30 days to assess the GE content.

## Preparation and Characterization of Ginger-Extract Transethosomal and Nontransethosomal Hydrogel Formulations

Hydrogel formulations were fabricated using cold injection as per D'Souza et al<sup>30</sup> with slight modification. Three gelling agents were investigated: NaAlg (4% w:v), hydroxypropyl methylcellulose (HPMC; 3% w:v), and CS (2% w:v). The contents of the gelling polymers were selected in accordance with preliminary experimental trials to produce hydrogel of acceptable appearance and uniformity. In brief, GE 0.3% w:v was mixed with an aqueous solution of each gelling agent to develop free GE hydrogels (nontransethosomal). To prepare GE transethosomal hydrogels, freshly prepared GE-loaded TRE suspension (selected formulation TRE3) equivalent to 0.3% w:w GE was mixed with an aqueous solution of each gelling agent (NaAlg 4% w:v, HPMC 3% w:v, and CS 2% w:v) and then the hydrogels were adjusted to an ultimate weight of 10 g under constant stirring on a magnetic stirrer until homogeneous hydrogel formulations were achieved. Finally, the fabricated transethosomal and nontransethosomal GE hydrogels were left in the fridge until further investigations. The composition of the hydrogel preparations is detailed in Table 1. The clarity, homogeneity, and phase separation of the preparations were examined visually.<sup>31</sup>

### Ginger-Extract Content and pH of Transethosomal and Nontransethosomal Hydrogel Formulations

The contents of GE in the TRE hydrogel preparations were determined via dissolving precisely weighed hydrogels (0.5 g) in ethyl alcohol to dissolve the vesicles and extract a quantity of drug. After the solution was filtered using filter paper, the drug content was determined using a UV-vis spectrophotometry at a maximum wavelength of 285 nm. The pH of GE hydrogel preparations was measured utilizing a 3500 pH meter (Jenway, UK).

### Viscosity of Ginger-Extract Transethosomal and Nontransethosomal Hydrogel Formulations

The viscosity of GE hydrogel formulations was determined using a Brookfield digital viscometer (DV-II, Brookfield Engineering Laboratories, Stoughton, MA) at 25°C. The viscosity measurements were detected using spindle number 96 at a shear rate of 15 rpm. The measurements were carried out in triplicate.<sup>31</sup>

### Rheological Behavior of Ginger-Extract Transethosomal and Nontransethosomal Hydrogel Formulations

Rheological analyses were carried out using the Brookfield digital viscometer. The viscosities of the hydrogel preparations were estimated at a range of shear rates (5–60 rpm) at room temperature using spindle number 96. The rheological property of the hydrogels was exhibited using the flow curve of the viscosity values versus shear rate.<sup>31</sup>

### Spreadability of Ginger-Extract Transethosomal and Nontransethosomal Hydrogel Formulations

The spreadability of the fabricated hydrogel formulations was evaluated employing a previously reported method.<sup>32</sup> Specific weight (2 g) of hydrogel was placed on a glass slide (7.5 cm in length). Another slide of the same length was kept on the top of the hydrogel such that the hydrogel was trapped between the two slides and expanded at a certain distance. A weight of 100 g was fixed on the upper slide for 10 min to evenly compress the gel to a constant thickness, preventing any further gel spreading. After that, the time needed for separation the slides was measured in seconds. Then, the spreadability was estimated:

$$S = \frac{M \times L}{T} \quad (3)$$

where  $S$  corresponds to spreadability (g.cm/s),  $M$  is weight fixed on the upper slide (100 g),  $L$  is the length of the utilized glass slides (7.5 cm), and  $T$  is the time consumed in seconds for complete separation of the slides. The measurements were performed in triplicate.

## In Vitro Release of Ginger Extract from Transethosomal and Nontransethosomal Hydrogel Formulations

In vitro release was carried out utilizing a dialysis membrane approach across a semipermeable cellophane membrane (molecular weight cutoff 12,000–14,000 Da, Sigma Aldrich, St Louis, MO, USA) as mentioned in a previous report with slight changes.<sup>6</sup> Briefly, 1 g samples of different GE transethosomal and nontransethosomal hydrogel formulations were precisely weighed and kept over dialysis semipermeable membrane previously soaked in PBS (pH 7.4 for 24 h) and fitted

over the lower-end opening of a glass tube of 2 cm diameter. These tubes were dipped in a 100 mL beaker containing PBS (pH 7.4). The system was kept at  $37^{\circ}\pm 0.5^{\circ}\text{C}$  in a thermostatically controlled shaking water bath (Daihan Scientific, Seoul, South Korea) rotating at 50 rpm. Samples of 5 mL were removed at predefined time intervals (0.5, 1, 2, 4, 6, 8, 12, and 24 h). Removed sample volumes were replaced by the same volume of freshly developed release medium at the same temperature to maintain sink conditions. The released content of GE was estimated by using UV-vis spectrophotometry at a maximum wavelength of 285 nm. The in vitro release of GE from selected GE-TRE3 dispersion and free ginger solution was studied for comparison. The in vitro drug release procedures were repeated in triplicate.

## Kinetic Analysis

The kinetics of drug release from the tested hydrogel formulations was studied using linear regression analysis. The in vitro release results were fitted in accordance with various kinetic models: zero order, first order, and Higuchi diffusion. A Korsmeyer–Peppas model was utilized to investigate the mechanism of drug release by plotting log cumulative percentage of drug released versus log time.<sup>33</sup> The value of the exponent (n) evaluating the mechanism of drug release is calculated from the slope of the straight line produced. Where exponent (n) is  $\leq 0.5$ , this corresponds to a Fickian diffusion mechanism, while  $0.5 < (n) < 1.0$  corresponds to a non-Fickian mechanism (anomalous diffusion). The non-Fickian diffusion indicates the combination of both diffusion and erosion-governed drug-release rate.

## Ex Vivo Skin Permeability and Deposition

Skin permeability of selected GE-TRE hydrogel (HPMC-TRE3), free GE hydrogel (HPMC-GE) formulations, and GE hydroalcoholic solution was examined using abdominal skin of male rats according to a previously reported method.<sup>34</sup> The experimental protocol was approved by members of the Research Ethics Committee and the head of Pharmacology and Toxicology Department, Faculty of Pharmacy, South Valley University, Egypt (PSVU 126/22). The animals were killed, then the dorsal side hairs of abdominal skin were removed with the aid of an electrical caliber. Then, the subcutaneous fat of the skin was washed three times with a cotton piece dipped in isopropyl alcohol. The skin was divided into appropriate-sized pieces and immersed in PBS (pH 7.4 for 4 h) to stabilize the skin membrane prior to the permeation experiment. Then, the skin was extended across the bottom open end of a glass tube of 2 cm diameter and immersed in a glass beaker containing 100 mL PBS and maintained in a vertical position such that the membrane was just below the surface of the solution. The donor (tubes) and receptor (beaker) were maintained at  $37^{\circ}\pm 0.5^{\circ}\text{C}$  in a thermostatically controlled shaking water bath rotating at 50 rpm. Tested preparations (0.5 g hydrogels, 0.5 mL drug solution) were placed on the skin (donor compartment). Aliquots of 5 mL were withdrawn from the receptor at predefined time intervals (up to 24 h) and replaced with freshly prepared release medium. The drug content was measured via employing UV-vis spectrophotometry at a maximum wavelength of 285 nm. Ex vivo permeation measurements were performed in triplicate. GE cumulative amount ( $\mu\text{g}$ ) permeated through unit area was plotted on a curve versus time. The flux ( $J$ ,  $\mu\text{g}\cdot\text{cm}^2/\text{s}$ ) and permeability coefficient ( $P_{app}$ ,  $\text{cm/s}$ ) of GE through skin membrane were estimated utilizing Fick's first law (Equations 4 and 5):

$$J = \frac{dQ}{A \cdot dt} \quad (4)$$

where  $dQ$  is change in drug amount ( $\mu\text{g}$ ) across the skin and  $A$  ( $\text{cm}^2$ ) the area of skin surface.

$$P_{app} = \frac{J}{C_0} \quad (5)$$

where  $C_0$  is the drug concentration at zero time ( $\mu\text{g/mL}$ ) in donor compartment.

## Stability of Selected Ginger-Extract Transethosomal Hydrogel

The stability of the selected GE-TRE hydrogel formulation (F6) was carried out during the storage period. The tested formulation was stored in a sealed 20 mL glass vial in the refrigerator (at  $4^{\circ}\pm 1^{\circ}\text{C}$ ) and at room temperature ( $25^{\circ}\pm 1^{\circ}\text{C}$ ) for

1 month. Then, the examined formulation was monitored for appearance, homogeneity, surface pH, spreadability, and viscosity. The stability study was conducted in triplicate.

## In Vivo Animal Studies

### Skin Irritation

Skin-irritation studies were conducted to prove that the GE and concentration of ingredients utilized for TRE development were safe and nonirritant to rat skin. The experimental procedures were carried out to assess any possible undesirable reaction of the GE formulation upon application on the skin surface of the rats in accordance with a technique described previously.<sup>35,36</sup> The animals were divided into three groups (n=3): negative control (no treatment), 0.3% free GE hydrogel, and treated with selected transthesosomal hydrogel (HPMC 3%-GE-TRE3). A dose of 1 g of GE hydrogel formulations was administered on a particular region of the shaved dorsal surface of the rats' skin daily for 3 days.<sup>37</sup> The skin was examined visually for the appearance of any sign of irritation or edema every day for 3 days. The examined skin was compared with positive-control rat skin irritated with formalin solution (0.8% v:v) as standard irritant.<sup>35</sup>

### Anti-Inflammatory Performance in Induced Paw-Edema Rat Model

The anti-inflammatory performance of the selected TRE hydrogel formulation was examined employing carrageenan-induced paw edema.<sup>38,39</sup> The experimental animals were divided into four groups, each containing five rats. Group 1 rats were used as negative controls and intraperitoneally injected with 1 mL of vehicle (normal saline). Group 2 (carrageenan) rats were injected with 0.1 mL carrageenan in saline (1% w:v) into the left hind paw to induce edema. Group 3 (treated with selected formulation) rats received transthesosomal HPMC hydrogel formulation (F6) containing 0.3% GE-loaded TREs prepared using sodium deoxycholate (GE-TRE3) prior to carrageenan injection in the same conditions as group 2. Group 4 (ketoprofen gel standard) rats were treated with ketoprofen (1%) gel as standard NSAID prior to carrageenan injection in the same conditions as group 2, with 0.5 g of the test formulation administered on edema paw tissue. The increment in paw thickness was determined using a Vernier caliper before the carrageenan injection, ie, at 0 h, and then at 1, 2, 3, 4, 5, 6, 7, and 8 h after carrageenan injection. The difference between paw thickness at 0 h and paw thickness at other times was used to calculate the increase in paw thickness. The detection of paw edema swelling and percentage inhibition of edema was carried out.

### TNF $\alpha$ Levels

Measurement of TNF $\alpha$  levels was carried out utilizing an ELISA kit for rat TNF (Biosource Europe, Belgium). Absorbance was measured using a plate reader (Spectra III, Austria) at wavelengths of 450 and 550 nm. TNF $\alpha$  level was then normalized to protein content after calculating the protein concentration.

### Prostaglandin E<sub>2</sub> Levels

PGE<sub>2</sub> was estimated employing an enzyme immunoassay (EIA) kit (Enzo Life Sciences, Switzerland). On a 96-well plate, goat antimouse IgG was utilized as a precoat before medium and PGE<sub>2</sub> EIA conjugate were added. The plate was subjected to a final wash to eliminate any last traces of the antibody-enzyme reagent, followed by 2 h of response time. The amount of PGE<sub>2</sub> present was measured in pg/mL, and the color intensity was detected at 405 nm.

### Oxidative Stress Parameters

Cold Krebs-HEPES buffer (10 mmol/L glucose, 0.02 mmol/L Ca-Tritriplex, 25 mmol/L NaHCO<sub>3</sub>, 1.2 mmol/L KH<sub>2</sub>PO<sub>4</sub>, 120 mmol/L NaCl, 1.6 mmol/L CaCl<sub>2</sub>, 1.2 mmol/L MgSO<sub>4</sub> 7H<sub>2</sub>O, and 5 mmol/L KCl, pH 7.4) was used to homogenize the paw tissues as previously mentioned.<sup>40</sup> Reactive oxygen species (ROS) generation was estimated in the presence of lucigenin, (5  $\mu$ mol/L). NADPH (100 mol/L) was added to initiate the reaction, and over the course of 30 minutes, relative light units (RLU) of the chemiluminescence were measured in a luminescent spectrometer (PerkinElmer). Results were adjusted to the protein content of each sample and presented as counts per minute.

## Histopathological Examination

Thin and thick serial paw-skin slices from paraffin blocks were acquired, processed, and ultimately stained with hematoxylin and eosin (H&E), then inspected under a light microscope (Optika Microsystems, Italy). Thin- and thick-skin specimens of each animal's inflammatory reaction intensity were graded: 0 = no inflammatory cells, 1 = inflammatory cells 10%, 2 = inflammatory cells 10%–50% and 3 = inflammatory cells >50%.<sup>41</sup> All histopathological changes were blindly carried out by a pathologist.

## Statistical Analysis

The experiments were carried at least thrice, and the findings are presented as means  $\pm$  SD. For statistical analysis, GraphPad Prism 8.4.3 (GraphPad, San Diego, CA) was utilized. Analysis was performed using one-way ANOVA with Tukey's test. Differences were considered statistically significant at  $P < 0.05$ .

## Results and Discussion

### Preparation of Transethosomes Loaded with Ginger Extract

TREs are a type of nanopatform that has the potential to greatly improve drug delivery to skin layers. GE was successfully loaded into TREs using a cold method to enhance the permeability and transdermal delivery of plant extract across the skin. Phospholipid was used for TRE development at concentration of 3% as bilayer-producing agent. Three types of edge activator were employed for the fabrication of GE-TREs at concentration of 0.3%. They were selected according to their values of hydrophilic lipophilic balance (HLB) to examine their effect on the physicochemical characteristics of the prepared nanovesicles. HLB values were 4.3, 15 and 18 for Span 80, Tween 80 and sodium deoxy cholate.<sup>42</sup>

### In Vitro Characterization of Transethosomes Loaded with Ginger Extract

#### Particle Size, $\zeta$ -Potential, Encapsulation Efficiency, and Drug Loading

Average particle sizes, polydispersity index,  $\zeta$ -potential, EE, and DL of GE-loaded TREs are listed in Table 2. The developed nanovesicles showed small particles and narrow polydispersity (PDI) of  $254.8 \pm 30.84$  nm,  $0.45 \pm 0.02$ ,  $286.23 \pm 10.54$  nm,  $0.327 \pm 0.012$ , and  $188.3 \pm 7.66$  nm,  $0.276 \pm 0.021$  (Figure 1B) using Span 80, Tween 80, and sodium deoxycholate as edge activators, respectively. The presence of sodium deoxycholate significantly ( $P < 0.05$ ) reduced the particle size when compared with other edge activators. This might be due to the anionic nature of sodium deoxycholate producing steric repulsion in nearby charged molecules that caused increase in curvature and reduced the size of vesicles.<sup>43</sup> The lower PDI values indicate the size uniformity and good homogeneity of the developed vesicles. A crucial aspect that might affect vesicular properties,  $\zeta$ -potential values can be used to partially suggest the stability of GE TREs. The continuous agglomeration of nanovesicles are dramatically reduced, and the stability is increased, attributed to electrostatic repulsion.<sup>42</sup> The  $\zeta$ -potential measurements illustrated that GE-loaded TREs fabricated using Span 80, Tween 80, and sodium deoxycholate had a value of  $-7.8 \pm 0.125$  mV,  $-21.1 \pm 0.265$  mV, and  $-38.6 \pm 0.08$  mV, respectively. As shown, GE-TREs prepared using deoxycholate exhibited significantly higher  $\zeta$ -potential when compared

**Table 2** Characterization of ginger extract (GE)-loaded transethosome (TRE) nanovesicles. Data presented as means  $\pm$  SD (n=3)

	Particle size (nm)	PDI	$\zeta$ -Potential (mV)	EE%	DL%
TRE1	$254.8 \pm 30.84$	$0.45 \pm 0.02$	$-7.8 \pm 0.125$	$79.26 \pm 0.60$	$7.67 \pm 0.04$
TRE2	$286.23 \pm 10.54$	$0.327 \pm 0.012$	$-21.1 \pm 0.265$	$84.81 \pm 0.73$	$8.20 \pm 0.04$
TRE3	$188.3 \pm 7.66^*$	$0.276 \pm 0.021$	$-38.6 \pm 0.08^*$	$91.0 \pm 0.24^*$	$8.8 \pm 0.03$

**Note:** \* $P < 0.05$  compared to TRE1 and TRE2.

**Abbreviations:** TRE1, GE-loaded TREs prepared using Span 80; TREs 2, GE-loaded TREs prepared using Tween 80; TRE3, GE-loaded TREs prepared using sodium deoxycholate; EE, encapsulation efficiency; DL, drug loading; PDI, polydispersity index.

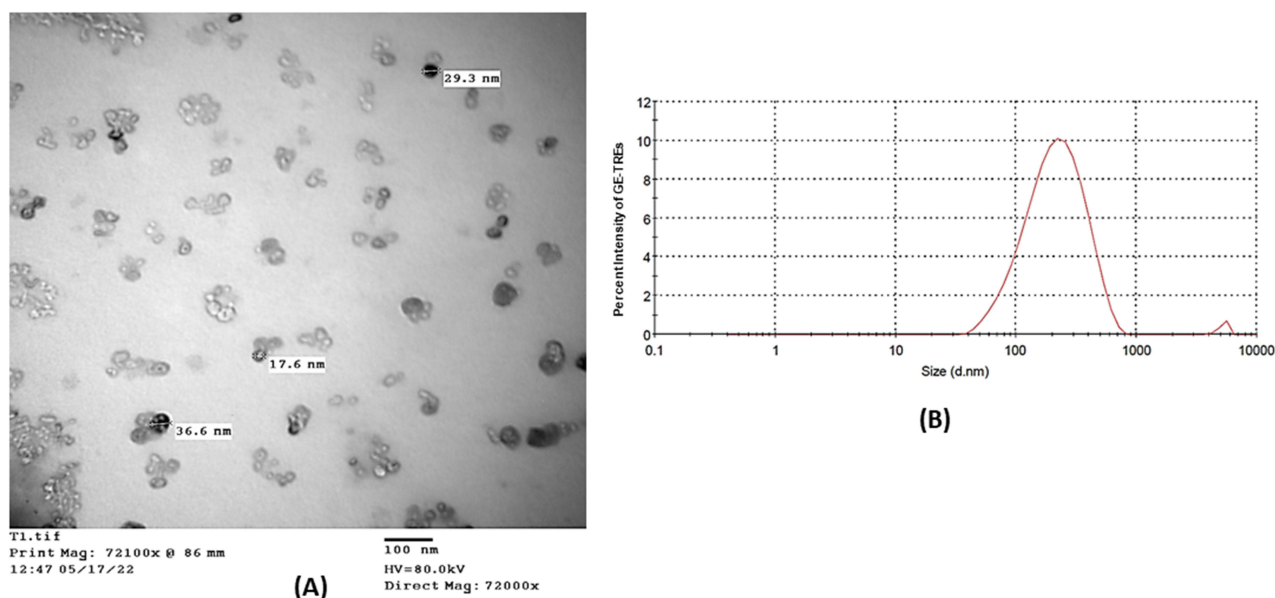


**Figure 1** (A) Transmission electron microscopy and (B) size distribution of GE-loaded transeosomes prepared using sodium deoxycholate. Magnification 72,000 $\times$ , scale bar 100 nm.

with Span 80 and Tween 80, which proved the stability of the vesicles and minimum electrostatic attraction avoiding vesicle aggregation. The TREs had EE of  $79.26\% \pm 0.60\%$ ,  $84.81\% \pm 0.73\%$ , and  $91.0\% \pm 0.24\%$  and DL of  $7.67\% \pm 0.04\%$ ,  $8.20\% \pm 0.04\%$ , and  $8.8 \pm 0.03\%$  for GE-TREs prepared using Span 80, Tween 80, and sodium deoxycholate, respectively. The significantly higher EE of GE-loaded TREs consisting of sodium deoxycholate may be related to the highly solubilizing characteristics and incorporation into the lipid bilayer, which enhances medication entrapment into nanovesicles. These findings are in accordance with previous work that revealed that the higher encapsulation of meloxicam and dexamethasone was obtained by employing sodium cholate as edge activator in the preparation of lipid nanovesicles.<sup>43,44</sup> Based on the previous experimental results, GE-loaded TREs prepared using sodium deoxycholate (TRE3) exhibited appropriate attributes in terms of higher EE, DL, smaller particles, and higher  $\zeta$ -potential than TREs prepared using Span 80 and Tween 80. Therefore, GE-loaded TREs comprised of sodium deoxycholate (TRE3) were selected for further studies and characterization.

### Transmission Electron Microscopy

Particle size and morphology of the prepared nanovesicles were monitored by TEM. Figure 1A demonstrates the photomicrograph of GE-loaded TREs (TRE3) prepared using sodium deoxycholate as edge activator. The vesicles are spherical and nonaggregated with uniform and homogeneous distribution. It was noticed that the average size on TEM imaging was  $28.83 \pm 7.19$  nm for the fabricated TREs. This is smaller than that produced by DLS measurements ( $188.3 \pm 7.66$  nm). This difference may be due to the dryness of the examined samples during TEM examination.<sup>45,46</sup>

### Fourier-Transform Infrared Spectroscopy Analysis

The FT-IR spectra of GE, blank TREs and GE TREs (TRE3) prepared using sodium deoxycholate are presented in Figure 2. The FT-IR spectra of pure GE (Figure 2, trace A) present the characteristic peaks of phenol products: a broad beak was found at  $3590\text{ cm}^{-1}$  due to hydrogen bond O–H stretching of hydroxyl groups. Bands at  $2928$  and  $2857\text{ cm}^{-1}$  corresponded to  $\text{CH}_2$  stretching peaks, bands at  $1374\text{ cm}^{-1}$ ,  $1268\text{ cm}^{-1}$ ,  $1100\text{ cm}^{-1}$ , and  $891\text{ cm}^{-1}$  corresponded to aromatic C–H stretching, –C–O–C stretching, and –C–O stretching of –C–O–H bonds. The characteristic peak of gingerol (main constituent of ginger) was observed at  $1642$ , which represented C=O.<sup>47–49</sup> The FT-IR spectra of the blank TREs (Figure 2, trace B) illustrated characteristic peaks of phosphatidylcholine at  $2920\text{ cm}^{-1}$ ,  $2854\text{ cm}^{-1}$  and  $1736\text{ cm}^{-1}$  corresponding to C–H stretches and carbonylic C=O stretch of ester, respectively. Also, the main characteristic peak of sodium deoxycholate in blank TREs (Figure 2, trace B) was shown at  $3405.10\text{ cm}^{-1}$  due to the aliphatic O–H stretch. In the spectrum of GE-TRE3 (Figure 2, trace

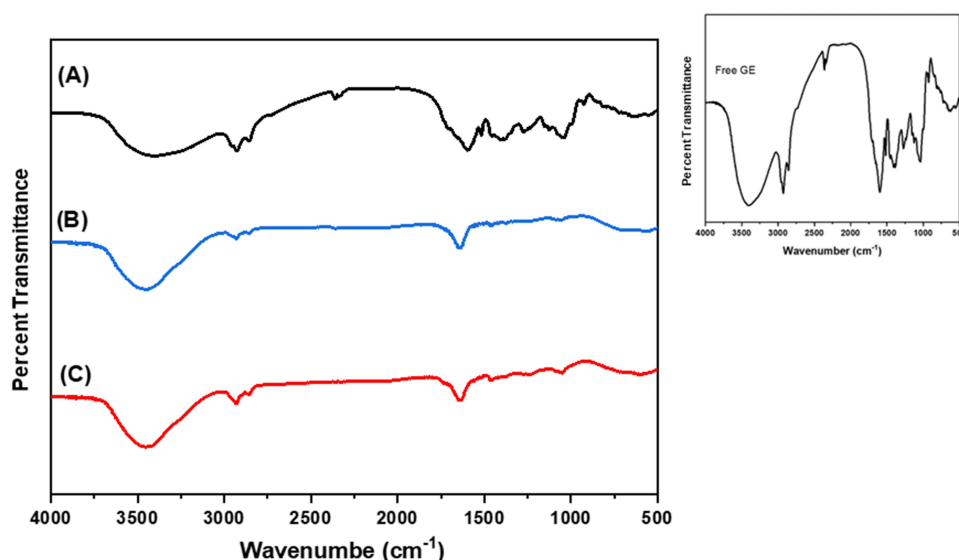


**Figure 2** FT-IR spectra of (A) pure ginger extract, (B) blank transethosomes, and (C) ginger-extract transethosomes prepared using sodium deoxycholate (TRE3).

(C) the broad peak ( $3590\text{ cm}^{-1}$ ) was shifted to lower wavelength. This may be due to the formation of a new hydrogen bond. In addition, it was noticed that the absorption peaks of GE at  $1268$ ,  $1100$  and  $891\text{ cm}^{-1}$  disappeared. These results may indicate the development of nanovesicles with appropriate shape, size, and better stability, as reported in a previous study.<sup>50</sup>

### Stability of the Selected Transethosomes Loaded with Ginger Extract

As shown in Table 3, GE TRE formulation prepared using sodium deoxycholate were found to be stable when stored at  $4^{\circ}\text{C}$  and  $25^{\circ}\text{C}\pm 1^{\circ}\text{C}$  for 1 month, they showed no sedimentation or aggregation. Moreover, the tested formulation exhibited a nonsignificant ( $P>0.05$ ) change in vesicle size and polydispersity when stored at  $4^{\circ}\text{C}$  and  $25^{\circ}\text{C}\pm 1^{\circ}\text{C}$ . In addition, GE-TRE formulation stored at these temperatures showed an improved chemical stability because of the GE content being maintained during storage. The results revealed that TREs protected GE from degradation and improved stability. Verma et al<sup>51</sup> proved that encapsulating drug products into nanovesicles is a promising approach to improve their stability. This is due to the opportunity of these nanosystems to protect the drug products inside the core, preventing them from being exposed to the environment.

### Preparation and Characterization of Ginger-Extract Transethosomal and Nontransethosomal Hydrogel Formulations

The visual detection of the developed GE gel formulations proved that the prepared hydrogels of free GE were clear and homogeneous. Also, GE-loaded TRE hydrogels presented slight opacity and good homogeneity and consistency without

**Table 3** Physical appearance, mean vesicle size, polydispersity index (PDI) and entrapment efficiency (EE) of GE-loaded TREs after 1-month storage at  $4^{\circ}\text{C}$  and  $25^{\circ}\text{C}$ . Data presented as means  $\pm$  SD ( $n=3$ )

	Zero time		30 Days	
	$4^{\circ}\text{C}$	$25^{\circ}\text{C}$	$4^{\circ}\text{C}$	$25^{\circ}\text{C}$
Visual appearance	No sedimentation	No sedimentation	No sedimentation	No sedimentation
EE%	$91.0\pm 0.24$	$91.0\pm 0.24$	$89.16\pm 0.42^{\text{NS}}$	$89.10\pm 0.9^{\text{NS}}$
PDI	$0.276\pm 0.04$	$0.276\pm 0.04$	$0.321\pm 0.03$	$0.34\pm 0.021$
Size (nm)	$188.3\pm 7.66$	$188.3\pm 7.66$	$210.21\pm 10.63$	$215.41\pm 13.18$

Abbreviation: NS, not significant.

**Table 4** Characterization of ginger extract transethosomal and nontransethosomal hydrogel formulations. Results presented as a means  $\pm$  SD (n=3)

	pH	Viscosity (mPa)	Clarity	Homogeneity	Drug content	Spreadability (g.cm/s)	Skin irritation
F1	7.0 $\pm$ 0.05	3666.66 $\pm$ 208.0	Clear	Good	99.1 $\pm$ 1.2	7.63 $\pm$ 0.23	Null
F2	6.9 $\pm$ 0.03	2500 $\pm$ 189.0	Clear	Good	99.0 $\pm$ 0.98	8.51 $\pm$ 0.18	Null
F3	7.2 $\pm$ 0.06	1800 $\pm$ 190.0	Clear	Good	99.1 $\pm$ 1.12	9.95 $\pm$ 0.40	Null
F4	7.1 $\pm$ 0.03	6100 $\pm$ 232.0*	Slightly opaque	Good	98.0 $\pm$ 0.95	9.83 $\pm$ 0.67	Null
F5	7.1 $\pm$ 0.05	4700 $\pm$ 153.17*	Slightly opaque	Good	97.6 $\pm$ 0.93	12.6 $\pm$ 0.16	Null
F6	7.0 $\pm$ 0.07	4000 $\pm$ 325.38*	Slightly opaque	Good	99.4 $\pm$ 1.21	13.71 $\pm$ 0.17	Null <sup>#</sup>

**Notes:** \* $P < 0.05$  (transethosomal hydrogel vs nontransethosomal hydrogel); <sup>#</sup>skin irritation evaluated visually after application of the tested formulations in comparison with irritated skin in positive-control rats that received formalin 0.8% v/v as reference irritant for 3 days.

any lumps or air bubbles. The pH values of GE transethosomal and nontransethosomal hydrogels were in the range of 6.9–7.2 (Table 4), which might not produce irritation. Therefore, they were considered appropriate for skin application.

GE content in the fabricated hydrogel formulations ranged from 97.6% $\pm$ 0.93% to 99.4% $\pm$ 1.21% (Table 4). This proved the high homogeneity of the developed hydrogel formulations. Spreadability is considered a crucial parameter in patient enforcement and helps in homogeneous administration of hydrogel to the skin or inflamed area. An appropriate hydrogel that has elegant spreadability spreads easily via minimum shear. As illustrated in Table 4, The spreadability values ranged from 7.63 $\pm$ 0.23 to 13.71 $\pm$ 0.17 g.cm/s. The spreadability of GE-loaded TRE hydrogels exhibited significantly higher spreadability than hydrogel formulations containing free GE. Our findings in this work are in agreement with the results of a previous study.<sup>52</sup>

As shown in Table 4, the developed GE TRE hydrogels prepared using different edge activators exhibited significantly ( $P < 0.05$ ) higher viscosity values than the free GE hydrogels at constant shear rate 15 rpm. The increased viscosity of the transethosomal gel might be related to the effect of TRE lipid bilayer vesicles prepared using Span 80, Tween 80, and sodium deoxycholate compared with hydrogel contacting free GE. These results revealed that the incorporation of TRE vesicles into the hydrogel system might offer enhanced stability and transdermal drug delivery due to drug protection and retardation of vesicle fusion.<sup>9,53</sup> Generally, higher values of viscosity and spreadability of transethosomal hydrogels improve transdermal delivery of GE across the skin.

Rheological properties of the prepared GE transethosomal and nontransethosomal hydrogel formulations (F1, F2, F3, F4, F5 and F6) were evaluated. The observations of viscosity for each hydrogel formulation at different shear rates are presented in Figure 3. It was observed that all the hydrogel formulations showed shear rate-thinning behavior with thixotropy (pseudoplastic

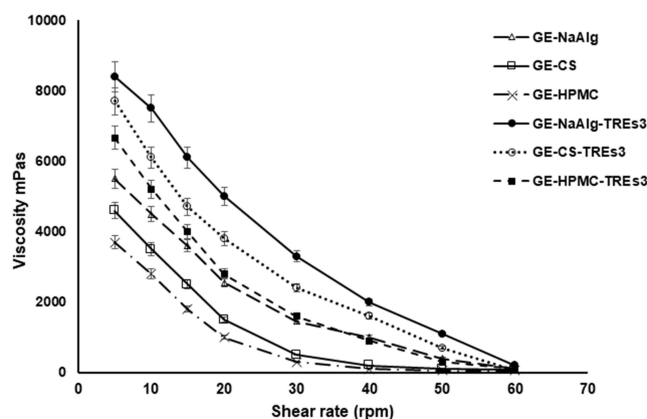


**Figure 3** Rheological profiles of GE transethosomal and nontransethosomal hydrogel formulations at 25°C (n=3).

fluid characteristics). Thixotropy means decreasing viscosity with an increase in shear rate and is a crucial characteristic for topical and transdermal application<sup>31</sup>. The pseudoplastic behavior possesses controlled drug release and appropriate application of the hydrogel on the affected skin area compared to Newtonian fluid.<sup>52</sup> The prepared GE-loaded TRE hydrogel formulations have acceptable thixotropy and viscosity and offer a promising transdermal delivery system.

## In Vitro Release of Ginger Extract from Transethosomal and Nontransethosomal Hydrogel Formulations

Cumulative GE released from different hydrogel preparations containing three investigated gelling agents (F1, F2, F3, F4, F5, and F6) was conducted in PBS (pH 7.4 at 37°C) utilizing dialysis membrane diffusion. The release profiles of GE from hydrogel formulations (F1, F2 and F3) compared with free GE hydroalcoholic solution are depicted in **Figure 4A**. Also, release profiles of GE from TRE hydrogel formulations (F4, F5 and F6) were compared with GE-loaded TRE suspension (**Figure 4B**). It was observed that free GE solution exhibited a significant higher amount of drug released ( $P < 0.05$ ) after 2 h ( $72.22\% \pm 0.28\%$ ) compared with GE hydrogels. This was probably due to the existence of gelling agents that performed as a resistant barrier to drug release because of their viscosity. It was reported that water migration into the gelling network and the diffusion of drug through the swelled matrix regulate and control drug release from hydrogel formulations.<sup>9</sup> Similar conclusions were reported by Khurana et al,<sup>54</sup> who found that meloxicam was released in a controlled pattern from hydrogel formulation compared to meloxicam solution. HPMC hydrogel formulation of GE demonstrated a significant higher drug release of 58.4% after 2 h when compared with CS hydrogel (47.5%) and NaAlg (26.1%) after the same time (**Figure 4A**). Then, HPMC hydrogel exhibited 92% of the drug that was released after 24 h. This result is related to the variations of the employed gelling agents' structure and viscosity, as well as the difference in interaction between drug and gelling polymer. As observed in the viscosity results, the hydrogel with lower viscosity presented higher GE release as obtained from hydrogel containing HPMC (F3), while those with higher viscosity showed lower percentage of drug release. These observations are consistent with the results observed in previous reports.<sup>55,56</sup> Regarding the hydrogel of GE-loaded TREs (**Figure 4B**), the highest release percentages at all time intervals were observed in HPMC (F6), followed by CS (F5) then sodium alginate (F4) hydrogel matrix. This was probably due to the highest viscosity of sodium alginate and possible attraction between negatively charged TREs and cationic CS hydrogel network, which consequently limit drug release.<sup>52</sup>

**Figure 5** shows that the GE-loaded TRE dispersion displayed an initial burst drug release of 27% during the first 2 h, then a slow sustained drug release (87.4%) over 24 h. The release profile of GE from the TRE dispersion exhibited a significantly slower release pattern than free GE incorporated in HPMC hydrogel (F3) (50% after 2h), probably as a result of the rigidity of the lipid bilayer membrane.<sup>7</sup> Further, the cumulative amount of GE released from TREs incorporated into the HPMC hydrogel (F6) was found to be 20% within 2 h, then a sustained release rate of 80% drug was observed over 24 h. The slower release

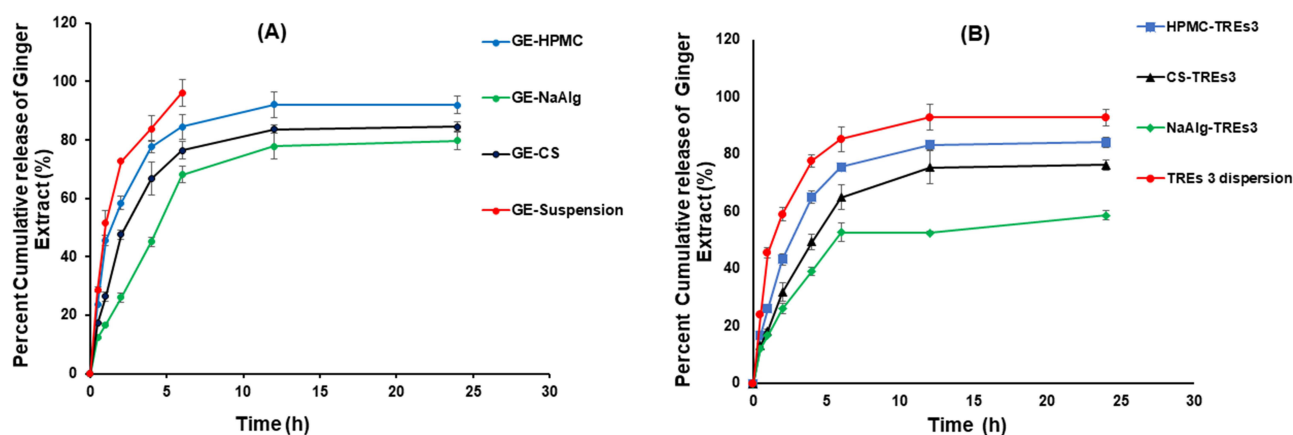


**Figure 4 (A)** Cumulative in vitro release profiles of GE from NaAlg hydrogel (F1), CS hydrogel (F2), HPMC hydrogel (F3), and GE aqueous solution in phosphate buffer (pH 6.8 for 24 h at 37°C). Data presented as means  $\pm$  SD (n=3). **(B)** Cumulative in vitro release profiles of GE from NaAlg TRE3 hydrogel (F4), CS-TRE3 hydrogel (F5), HPMC-TRE3 hydrogel (F6), and GE-TRE3 suspension in phosphate buffer (pH 6.8 for 24 h at 37°C). Data presented as means  $\pm$  SD (n=3).

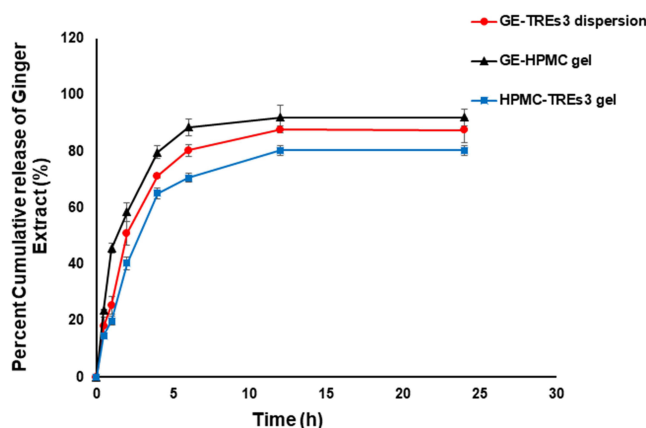


**Figure 5** Cumulative in vitro release profiles of GE from TRES3 dispersion, HPMC hydrogel (F3), and HPMC-TRE3 hydrogel (F6) in phosphate buffer (pH 7.4 for 24 h at 37°C). Data presented as means  $\pm$  SD (n=3).

when compared with TREs dispersion and free drug hydrogel probably related to drug diffusion through the TRE lipid bilayer vesicles and followed throughout the matrix network of the aqueous hydrogel.<sup>57</sup> The previous results proved that the TRE hydrogel system offered a sustained release pattern of GE when administered transdermally.

## Kinetic Analysis

To investigate the mechanisms regulating drug release from the different formulations, the results of the release study were analyzed using three kinetic models (zero-order, first-order, and Higuchi diffusion kinetic models) based on correlation coefficients ( $R^2$ ) and release-rate constants ( $K$ ) for different mathematical models. The results revealed that GE release from all investigated formulation was best fitted to Higuchi diffusion because of the higher values of correlation coefficients (0.922 $\pm$ 0.015, 0.873 $\pm$ 0.014, 0.845 $\pm$ 0.021, 0.904 $\pm$ 0.038, 0.915 $\pm$ 0.017, and 0.910 $\pm$ 0.014 for F1, F2, F3, F4, F5 and F6, respectively) compared to those obtained from zero (0.823 $\pm$ 0.011, 0.747 $\pm$ 0.021, 0.722 $\pm$ 0.034, 0.801 $\pm$ 0.024, 0.807 $\pm$ 0.028 and 0.785 $\pm$ 0.014 for F1, F2, F3, F4, F5, and F6, respectively) and first-order kinetics (0.877 $\pm$ 0.014, 0.809 $\pm$ 0.012, 0.843 $\pm$ 0.027, 0.835 $\pm$ 0.021, 0.859 $\pm$ 0.031, 0.843 $\pm$ 0.013, and 0.840 $\pm$ 0.020 for F1, F2, F3, F4, F5, and F6, respectively). In addition, the release data were fitted to the Korsmeyer–Peppas model and the value of ( $n$ ) calculated. All the GE hydrogel preparations displayed ( $n$ ) values of  $0.5 < n < 1.0$ , (0.545 $\pm$ 0.014, 0.727 $\pm$ 0.009, 0.646 $\pm$ 0.012, 0.503 $\pm$ 0.054, 0.695 $\pm$ 0.074, and 0.762 $\pm$ 0.039 for F1, F2, F3, F4, F5, F5, and F6, respectively) that corresponded to anomalous (non-Fickian) diffusion, meaning that the release of drug from the prepared formulations may be controlled by diffusion mechanism from the hydrogel network and partitioning through the lipid bilayer of TRE vesicles.<sup>52</sup> These findings are in accordance with previous research that found similar release profiles for TRE vesicles.<sup>52,56,58</sup>

## Ex Vivo Skin-Permeability and -Deposition Studies

The study of permeability of GE across the skin from the optimum transethosomal HPMC hydrogel (F6) in comparison with free GE HPMC hydrogel (F3) and GE solution was carried out for 24 h at 37°C. The results of the permeability profiles are presented in Figure 6A. The observed results revealed that TRE hydrogel formulation (F6) exhibited a significantly ( $P < 0.0001$ ) higher amount of GE permeated (436.55 $\pm$ 19.79  $\mu\text{g}\cdot\text{cm}^2$ ) after 24 h compared to 377.80 $\pm$ 10.06  $\mu\text{g}\cdot\text{cm}^2$  and 179.28 $\pm$ 14.16 obtained from nontransethosomal HPMC hydrogel (F3) and free GE solution, respectively. Moreover, transethosomal hydrogel displayed a significantly ( $P < 0.0001$ ) higher value of flux than those obtained from free drug hydrogel and free drug solution. The significantly highest ( $P < 0.0001$ ) mean apparent permeability coefficient ( $P_{app}$ ) of GE was obtained with the TRE3 HPMC hydrogel formulation (F6) (2.43 $\pm$ 0.008 $\times 10^{-6}$  cm/sec). The results showed that steady-state flux ( $J_{ss}$ ) from F6 was 3.35- and 2.1-fold higher than free drug solution and free drug hydrogel, respectively.

Higher GE skin deposition and permeation are probably due to the structure and nature of the nanosized TRE vesicles.<sup>59</sup> They can squeeze themselves into the stratum corneum and tiny pores in the skin. The enhanced skin delivery of this nanopatform may also be explained by the presence of ethanol and edge activator as permeation enhancer.

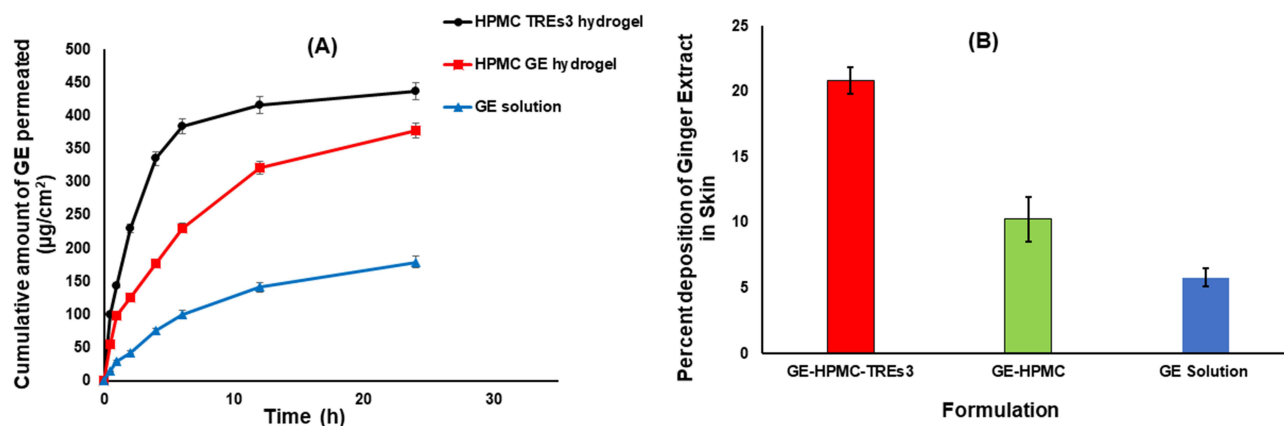


**Figure 6** Ex vivo permeation profiles (A) and skin-deposition percentages (B) of ginger extract HPMC hydrogel (F3) and HPMC-TRE3 hydrogel (F6) in comparison with drug solution in phosphate buffer (pH 7.4 for 24 h at 37°C). Data presented as means  $\pm$  SD (n=3).

Moreover, the phospholipid bilayer vesicles containing ethanol might have the potential to boost vesicle flexibility, enabling them to alter the structure of stratum corneum, penetrate the skin layer deeply and feasibly improve drug permeation.<sup>58,60</sup> Additionally, the nanosized TREs offered a higher area for drug penetration through the skin, resulting in a high level of drug concentration at the site of application (inflamed area). These findings indicate the promise of these TRE nanovesicles to facilitate drug penetration to deep layers of rat skin compared to the free drug.<sup>11</sup>

Figure 6B displays higher skin deposition of 20.87% of HPMC-TRE3 (F6) hydrogel compared to 10.25% and 5.81% of free GE HPMC hydrogel (F3) and GE solution, respectively. This outcome may be because of the synergetic impact of ethanol and edge activator association. The higher deposition revealed that GE-TRE hydrogel accumulated for an extended period in the skin, acting as a reservoir and enabling a prolonged performance of GE at the adjacent tissue of the deep layers of the skin during intervals between administrations.<sup>59,61</sup> Based on previous experimental results, it was concluded that the presence of an edge activator, ethanol, and phospholipid in the TRE nanosystem markedly improved GE permeation and skin deposition when compared to that of both drug solution and GE plain hydrogel.

## Stability of Selected Ginger-Extract Transethosomal Hydrogel Formulation

The stability study for the selected TRE hydrogel formulation (F6) was conducted at  $4^{\circ}\pm 1^{\circ}\text{C}$  and  $25^{\circ}\pm 1^{\circ}\text{C}$  for 1 month to investigate the storage stability of the formulation (Table 5). After 30 days, no significant changes were detected in surface pH, viscosity, drug content, homogeneity, or spreadability between the two storage temperatures. The selected TRE hydrogel formulation was found to be stable when stored at room temperature or in a refrigerator. This finding confirms the potentiality of the TRE nanovesicles to enable physical and chemical stability of GE hydrogel preparation.

**Table 5** Physicochemical evaluation of ginger extract transethosome hydrogel (HPMC-TRE3 gel; F6) during the stability study (means  $\pm$  SD, n=3)

	Zero time		30 Days	
	4°C	25°C	4°C	25°C
Storage temperature	4°C	25°C	4°C	25°C
Surface pH	7.0 $\pm$ 0.07	7.0 $\pm$ 0.07	7.1 $\pm$ 0.02	7.13 $\pm$ 0.06
Viscosity (mPa.S) (pH 7.4, 37°C)	4000 $\pm$ 325.38	4000 $\pm$ 325.38	3800 $\pm$ 225.18 <sup>NS</sup>	3650 $\pm$ 135.10 <sup>NS</sup>
Visual appearance	Homogeneous	Homogeneous	Homogeneous	Homogeneous
Drug content	99.4 $\pm$ 1.21	99.4 $\pm$ 1.21	98.4 $\pm$ 0.51 <sup>NS</sup>	98.1 $\pm$ 1.72 <sup>NS</sup>
Spreadability (g.cm/s)	13.71 $\pm$ 0.17	13.71 $\pm$ 0.17	12.51 $\pm$ 0.23	11.90 $\pm$ 0.21

Notes: NS, not significant compared to measurements at zero time ( $P>0.05$ ).

## In Vivo Animal Studies

### Skin Irritation

The study of skin irritation was carried out to confirm the safety and compatibility of the GE hydrogel formulations when applied to the skin of rats without any visible irritation. The results revealed that GE transethosomal (F6) and nontransethosomal hydrogel (F3) formulations exhibited zero scores (null irritation) when compared with highly irritated skin that received formalin solution as standard irritant. This finding indicate that the prepared GE hydrogel formulations (F3 and F6) are nonirritant and safe on rat skin.

### Anti-Inflammatory Performance in Induced Paw-Edema Rat Model

In this study, the anti-inflammatory effect of a novel GE transethosomal hydrogel was investigated against paw edema in adult rats induced by carrageenan compared to free GE hydrogel and reference ketoprofen gel (1%). The pharmacodynamic performance of GE hydrogel formulations in terms of anti-inflammatory efficacy on edema in hind paws of the rats is illustrated in Figure 7A and B, showing the edema swelling for up to 8 h and edema-inhibition percentages exhibited by the groups receiving free GE-HPMC (F3), GE-HPMC-TREs (F6) and marketed ketoprofen hydrogel formulations. Generally, a significant reduction in percentage of induced edema swelling was presented with the treated groups compared with the untreated group (Figure 7A). The group treated by hydrogel formulation F6 of GE TREs (TRE3, contains sodium deoxycholate) exhibited significantly ( $P<0.05$ ) higher percentage of edema inhibition (Figure 7B) compared with free GE HPMC hydrogel (F3) and reference ketoprofen gel. After 2 h, F6 showed  $66.11\% \pm 1.23\%$  edema inhibition compared to  $40.50\% \pm 1.72\%$  from F3. After 5 h, F6 displayed significant ( $P<0.05$ ) inhibition ( $86.34\% \pm 1.72\%$ ) of the induced edema compared to both F3 and ketoprofen gel 1%. The previous observations revealed superior anti-inflammatory activity of F6 compared to F3. This result matches the GE permeation study that demonstrated association between the higher percentages of GE transport across the skin and superior in vivo anti-inflammatory performance. These findings proved that transethosomal gel offered sustained and higher anti-inflammatory efficacy for a prolonged time when compared with free drug hydrogel. The prolonged anti-inflammatory effect exhibited by TRE hydrogel over free GE hydrogel is probably due to the nature of TRE nanovesicles, which act as a penetration enhancer. Also, they act as a nanosized drug vehicle that improves drug penetration, resulting in improved anti-inflammatory activity for prolonged time.

These findings are in accordance with those obtained by Salem et al, who investigated the anti-inflammatory effects of dapoxetine HCl transethosomal hydrogel transdermal delivery.<sup>52</sup> Previous reports investigated the in vivo anti-inflammatory performance of pure GE extracts when administered orally or parenterally.<sup>62,63</sup> Topical administration of GE was studied by Priprem et al,<sup>4</sup> who found that ginger-loaded niosomal gel achieved enhanced skin permeation and

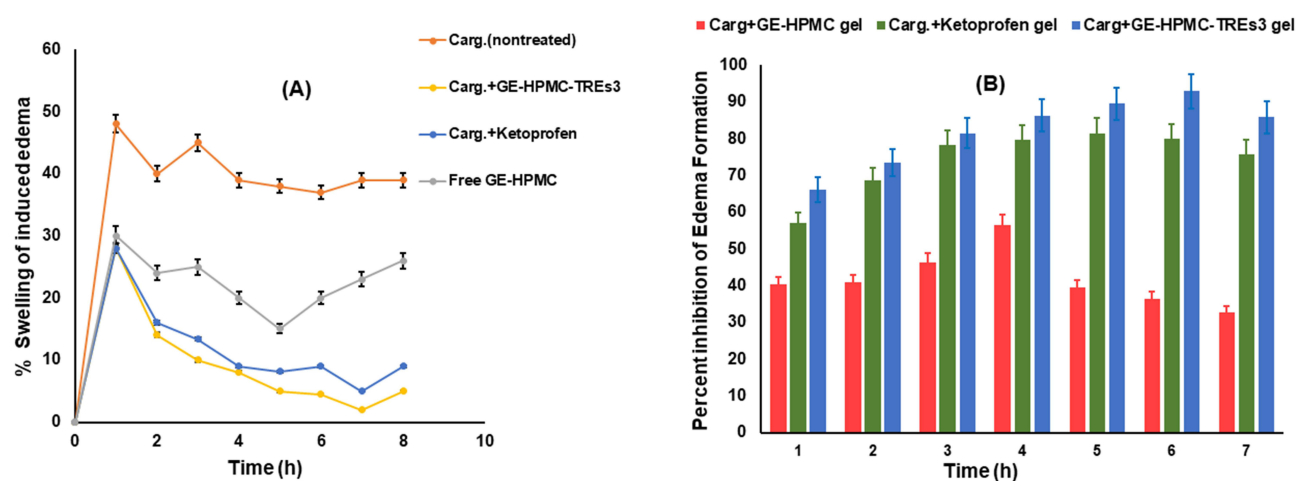


**Figure 7** Percentage swelling (A) and inhibition of induced paw edema (B) in rats after treatment with free ginger-extract HPMC hydrogel (F3), transethosomal HPMC hydrogel (F6), and commercial gel (ketoprofen, 1%) compared with unmedicated group (carrageenan-induced paw edema). \*Significantly different from free ginger-extract HPMC hydrogel (GE-HPMC) at  $P<0.05$ . Data presented as means  $\pm$  SEM of five experimental rats per group.

anti-inflammatory activity against ear edema induced by croton oil in mice. In our investigation, a novel nanopatform, TRE hydrogel, was successfully developed as a transdermal delivery system presenting sustained and improved anti-inflammatory effects of GE. It is known that upon carrageenan injection, levels of  $\text{TNF}\alpha$ ,  $\text{PGE}_2$ , and reactive oxygen species (ROS) are elevated in inflammatory conditions. Therefore, the levels of these inflammatory mediators were estimated in the animal groups that were treated with GE-HPMC-TRE3 gel and commercial ketoprofen gel compared with untreated and normal control animal groups.

### $\text{TNF}\alpha$ and Prostaglandin $\text{E}_2$ Levels

$\text{TNF}\alpha$  is a cytokine that has a crucial role in both acute and chronic inflammatory disorders. In this study, it was found that the serum  $\text{TNF}\alpha$  level was markedly increased in carrageenan-induced paw edema (untreated rat group) when compared to the normal control rats. The group that was treated with either GE-HPMC-TRE3 or ketoprofen commercial gel showed significantly ( $P < 0.05$ ) attenuated levels of  $\text{TNF}\alpha$  (Figure 8A). The level of  $\text{PGE}_2$  was estimated for animal groups and the results are presented in Figure 8B. There was a significant increase in serum  $\text{PGE}_2$  in the untreated group (carrageenan-induced paw edema) compared to the normal control rats. However, the treatment of rats with either HPMC-TRE3 or ketoprofen gel significantly ( $P < 0.05$ ) inhibited these changes (Figure 8B). This may be attributed to the inhibitory effect of GE on the release of different inflammatory

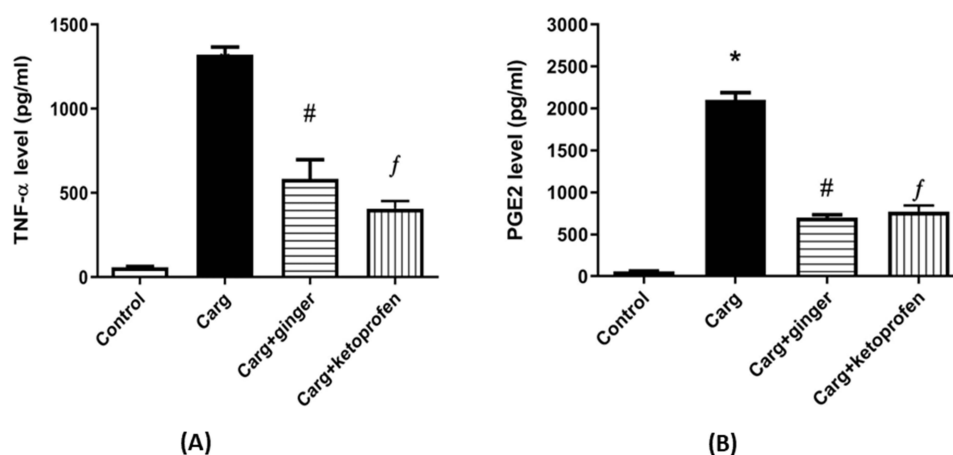


**Figure 8 (A)** Effect of GE-HPMC-TRE3 hydrogel and ketoprofen gel (1%) on serum  $\text{TNF}\alpha$  level in paw tissue. Means  $\pm$  standard errors of the mean (SEM). \* $P < 0.05$ , carrageenan vs control group; # $P < 0.05$ , carrageenan + GE-HPM-TREs and carrageenan ketoprofen group vs carrageenan group. **(B)** Effect of GE-HPMC-TRE3 hydrogel and ketoprofen gel (1%) on serum  $\text{PGE}_2$  level in paw tissue. Data presented as means  $\pm$  SEM. \* $P < 0.05$ , carrageenan vs control group; # $P < 0.05$ , carrageenan + GE-HPM-TREs and carrageenan + ketoprofen group vs carrageenan group.

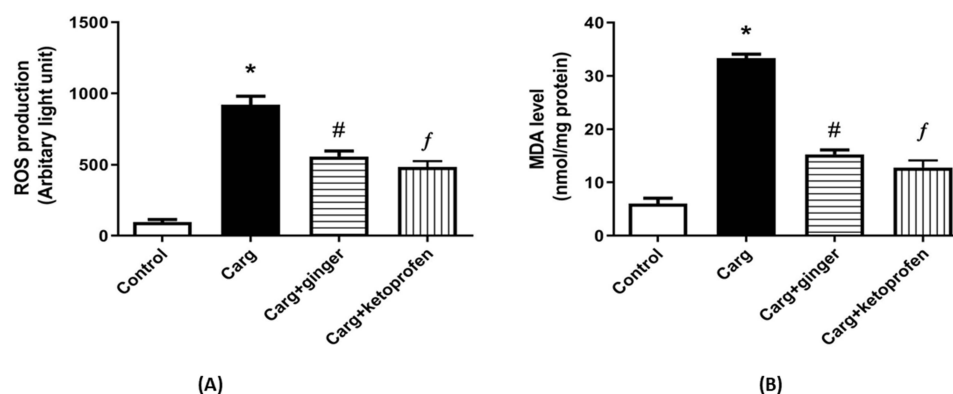


**Figure 9 (A)** ROS production in paw tissue in carrageenan-induced edema group was increased in compared with the control rats. GE-HPMC-TRE hydrogel and ketoprofen gel produced a significant decrease in ROS production compared to the control. **(B)** Paw-tissue homogenates of carrageenan-treated group showed a significant increase in MDA, and treatment with GE-HPMC-TRE hydrogel and ketoprofen gel inhibited this effect.

**Notes:** Values represent means  $\pm$  SEM.  $P < 0.05$ , carrageenan group vs control group; # $P < 0.05$ , carrageenan + GE-HPMC-TREs and carrageenan + ketoprofen groups vs carrageenan group.

mediators during inflammation reaction. GE consists of a variety of flavonoid active constituents that exert anti-inflammatory effects by inhibition of cyclooxygenase, as reported previously. These findings revealed the improved anti-inflammatory efficacy of GE when loaded into a nanosized TRE hydrogel formulation.

### Oxidative Stress Parameters

Elevation of ROS at the inflammation area is considered the main cause of tissue damage in many inflammatory disorders. The free radicals produced can stimulate inflammatory reactions, resulting in the increase of proinflammatory cytokines, which might lead to tissue damage. In this work, the paw edema induced via carrageenan in rats showed a marked increase ( $P < 0.05$ ) in ROS production compared to the control. Rats that were treated with either GE-HPMC-TRE3 or ketoprofen exhibited reduction in the levels of ROS (Figure 9A). Untreated rats, which received only

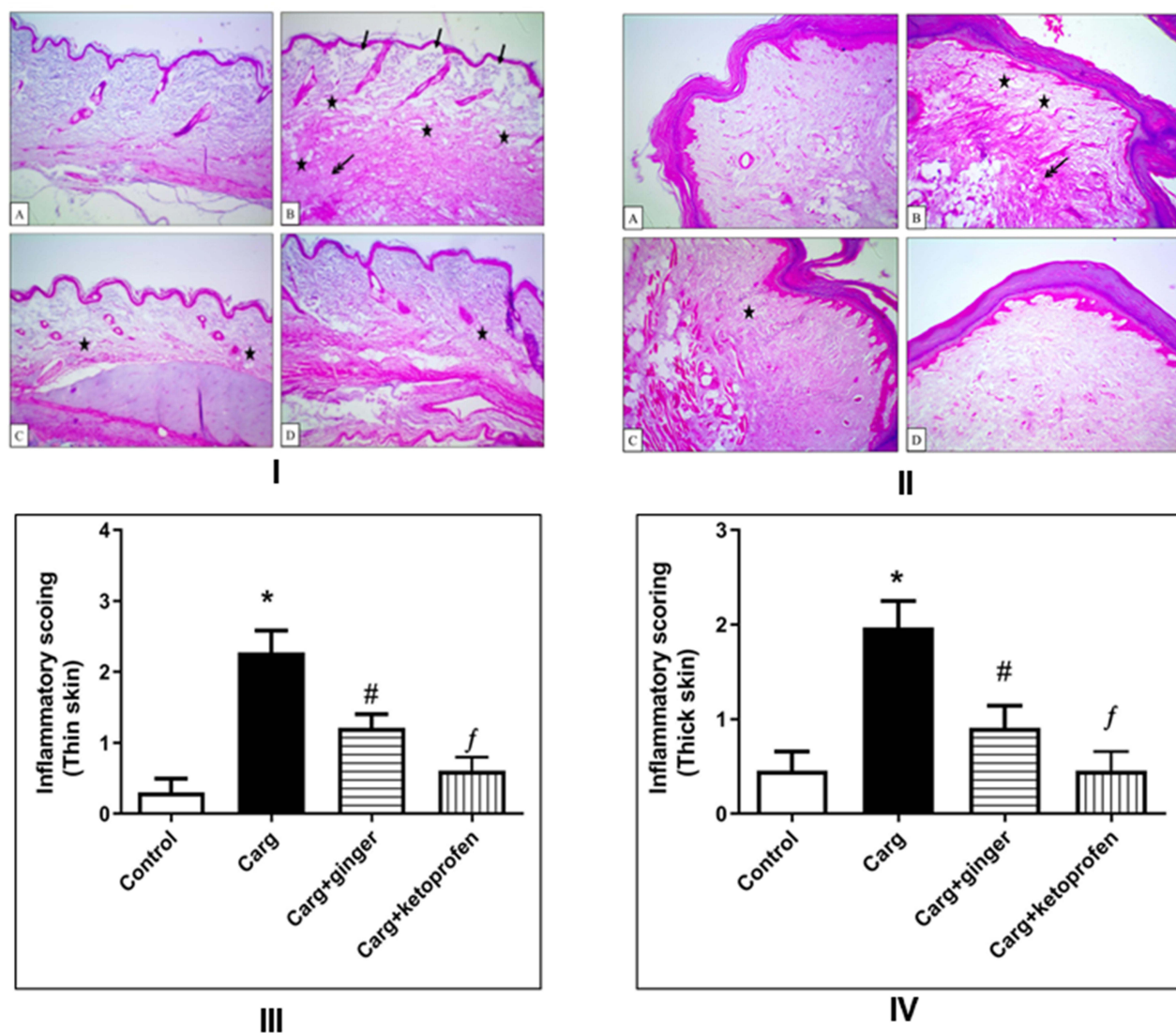


**Figure 10** I and II: Histological examination (H&E, 100×) of rat-paw skin. Histological examination of paw skin in rat model of carrageenan-induced paw edema using H&E staining. (I) Thin-skin photomicrographs; (II) thick-skin photomicrographs. IA and IIA: Control sections with normal histological structure in both thin and thick skin. IB and IIB: Sections obtained from positive control (carrageenan-induced edema without treatment) with detachment of epidermal layer (arrow), severe vacuolation, and edematous reaction in thin and thick skin (stars) and severe dermal inflammatory reaction in thin skin (double-headed arrow), as well as severe inflammatory reaction in dermal and muscular layers in thick skin (double-head arrow). IC and IIC: Sections obtained from animals treated with GE-HPMC-TRE3 hydrogel showed moderate dermal edematous and inflammatory reactions (stars). ID and IID: Sections obtained from animals pretreated with ketoprofen gel showed mild dermal edematous and inflammatory reaction (star). III and IV: Results of statistical analysis of inflammation scores of experimental groups for thin and thick skin.

**Notes:** (I) Thin skin and (II) thick skin. Values represent mean  $\pm$  SEM. \* $P < 0.05$ , carrageenan vs control group; # $P < 0.05$ , carrageenan + GE-HPMC-TRE3 and carrageenan + ketoprofen gel vs carrageenan group.

carrageenan, exhibited a significant increase ( $P<0.05$ ) in pancreatic MDA, while treatment with GE-HPMC-TRE3 hydrogel or ketoprofen gel inhibited this effect (Figure 9B).

### Histopathological Examination

Figure 10 I and II illustrate the histological examination of paw skin in the rat model of carrageenan-induced paw edema using H&E staining. (I) shows thin skin photomicrographs and (II) shows thick skin photomicrographs. IA and IIA represent normal control sections with normal histological structure in both thin and thick skin. IB and IIB represent sections obtained from positive control (carrageenan-induced edema without treatment) with detachment of epidermal layer (arrow), severe vacuolation and edematous reaction in thin and thick skin (star), and severe inflammatory reaction in the dermal tissue of thin skin (double-head arrow), as well as severe inflammatory reaction in dermal and muscular layers in thick skin (double-head arrow). IC and IIC sections obtained from animal pretreated with (GE-HPMC-TRE3 hydrogel) showed moderate dermal edematous and inflammatory reaction (star). ID and IID sections obtained from animal pretreated with (ketoprofen gel) showed mild dermal edematous and inflammatory reaction (star).

### Conclusion

In the current study, for the first-time GE was loaded into a new nanosystem called TREs to improve transdermal permeation and anti-inflammation effect. They were successfully fabricated using cold injection method and thoroughly characterized in terms of different parameters. The selected GE transethosomal dispersion containing sodium deoxycholate demonstrated high EE, acceptable DL, nanosized particles, and sustained drug release. The optimum transethosomal formulation was incorporated into an HPMC hydrogel system. GE transethosomal hydrogel was found to be appropriate for skin application and showed improved skin permeability as well as superior anti-inflammatory activity in the induced rat-paw edema model. In summary, TRE nanovesicles can be considered a very promising advanced nanovehicle able to be applied in the transdermal delivery of GE for the treatment of inflammation conditions. Nevertheless, stability studies for long-term storage are required in future work to evaluate and achieve pharmaceutical acceptability.

### Abbreviations

GE, ginger extract; TREs, transethosomes; HPMC, hydroxypropyl methylcellulose; CS, chitosan; ROS, reactive oxygen species.

### Ethics Approval

Experiments were conducted in accordance with the international ethical guidelines for animal care of the United States Naval Medical Research Centre, Unit 3, Abbaseya, Cairo, Egypt, accredited by the Association for Assessment and Accreditation of Laboratory Animal Care International. The procedures were in accordance with the *Principles of Laboratory Animal Care* (NIH publication 85-23, revised 1985). The study protocol was adopted by the Research Ethics Committee and the head of the Pharmacology and Toxicology Department, Faculty of Pharmacy, South Valley University, Egypt (PSVU 126/22).

### Acknowledgments

Many thanks to Professor Adel Baker (Department of Histology, Faculty of Veterinary Medicine, Cairo University) for help with histopathological examination.

### Author Contributions

All authors made a significant contribution to the work reported, whether in conception, study design, execution, acquisition of data, analysis, and interpretation, or all these areas, took part in drafting, revising, or critically reviewing the article, gave final approval to the version to be published, have agreed on the journal to which the article has been submitted, and agree to be accountable for all aspects of the work.

## Disclosure

The authors report no conflicts of interest in this work.

## References

1. Harirforoosh S, Asghar W, Jamali F. Adverse effects of nonsteroidal antiinflammatory drugs: an update of gastrointestinal, cardiovascular and renal complications. *J Pharm Pharm Sci*. 2013;16:821–847. doi:10.18433/J3VW2F
2. Zanfrescu A, Nitulescu G, Stancov G, et al. Evaluation of topical anti-inflammatory effects of a gel formulation with *Plantago lanceolata*, *Achillea millefolium*, *Aesculus hippocastanum* and *Taxodium distichum*. *Sci Pharm*. 2020;88:26.
3. Khoḡta S, Patel J, Barve K, Londhe V. Herbal nano-formulations for topical delivery. *J Herbal Med*. 2020;20:100300.
4. Priprem A, Janpm K, Nualkaew S, Mahakunakorn P. Topical niosome gel of *Zingiber cassumunar* Roxb. extract for anti-inflammatory activity enhanced skin permeation and stability of compound D. *AAPS PharmSciTech*. 2016;17:631–639.
5. Rodríguez-Luna A, Talero E, Ávila-Román J, et al. Preparation and in vivo evaluation of rosmarinic acid-loaded transethosomes after percutaneous application on a psoriasis animal model. *AAPS PharmSciTech*. 2021;22:1–18.
6. El-Mahdy MM, Hassan AS, El-Badry M, El-Gindy GE-DA. Performance of curcumin in nanosized carriers niosomes and ethosomes as potential anti-inflammatory delivery system for topical application. *Bull Pharm Sci*. 2020;43:105–122.
7. Ascenso A, Raposo S, Batista C, et al. Development, characterization, and skin delivery studies of related ultradeformable vesicles: transfersomes, ethosomes, and transethosomes. *Int J Nanomedicine*. 2015;10:5837.
8. Arora D, Nanda S. Quality by design driven development of resveratrol loaded ethosomal hydrogel for improved dermatological benefits via enhanced skin permeation and retention. *Int J Pharm*. 2019;567:118448.
9. Garg V, Singh H, Bhatia A, et al. Systematic development of transethosomal gel system of piroxicam: formulation optimization, in vitro evaluation, and ex vivo assessment. *AAPS pharmscitech*. 2017;18:58–71.
10. Ahad A, Aqil M, Kohli K, Sultana Y, Mujeeb M. Enhanced transdermal delivery of an anti-hypertensive agent via nanoethosomes: statistical optimization, characterization and pharmacokinetic assessment. *Int J Pharm*. 2013;443:26–38. doi:10.1016/j.ijpharm.2013.01.011
11. Chen Z, Li B, Liu T, et al. Evaluation of paeonol-loaded transethosomes as transdermal delivery carriers. *Eur J Pharm Sci*. 2017;99:240–245. doi:10.1016/j.ejps.2016.12.026
12. Albash R, Abdelbary AA, Refai H, El-Nabarawi MA. Use of transethosomes for enhancing the transdermal delivery of olmesartan medoxomil: in vitro, ex vivo, and in vivo evaluation. *Int J Nanomed*. 2019;14:1953. doi:10.2147/IJN.S196771
13. Jonathan VP, Maribel MCD. Potential use of transethosomes as a transdermal delivery system for metabolites from *Chenopodium murale*. *Materials Today Communicat*. 2022;30:103165.
14. Ramadan D, Pramesti SS, Anwar E. Formulation, stability test and in vitro penetration study of transethosomal gel containing green tea (*Camellia sinensis* L. Kuntze) leaves extract. *Int J Appl Pharm*. 2017;9:91–96. doi:10.22159/ijap.2017v9i5.20073
15. Moolakkadath T, Aqil M, Ahad A, et al. Development of transethosomes formulation for dermal fisetin delivery: box-Behnken design, optimization, in vitro skin penetration, vesicles-skin interaction and dermatokinetic studies. *Artif Cells Nanomed Biotechnol*. 2018;46:755–765. doi:10.1080/21691401.2018.1469025
16. El-Kady AM, Al-Megrin WAI, Abdel-Rahman IA, et al. Ginger is a potential therapeutic for chronic toxoplasmosis. *Pathogens*. 2022;11:798. doi:10.3390/pathogens11070798
17. Grzanna R, Lindmark L, Frondoza CG. Ginger—an herbal medicinal product with broad anti-inflammatory actions. *J Med Food*. 2005;8:125–132. doi:10.1089/jmf.2005.8.125
18. Dissanayake KGC, Waliwita W, Liyanage R. A review on medicinal uses of *Zingiber officinale* (ginger). *Int J Health Sci Res*. 2020;10:142–148.
19. Mashhadi NS, Ghiasvand R, Askari G, Hariri M, Darvishi L, Mofid MR. Anti-oxidative and anti-inflammatory effects of ginger in health and physical activity: review of current evidence. *Int J Prev Med*. 2013;4:S36.
20. Jolad SD, Lantz RC, Solyom AM, Chen GJ, Bates RB, Timmermann BN. Fresh organically grown ginger (*Zingiber officinale*): composition and effects on LPS-induced PGE2 production. *Phytochemistry*. 2004;65:1937–1954.
21. Shen C-L, Hong K-J, Kim SW. Comparative effects of ginger root (*Zingiber officinale* Rosc.) on the production of inflammatory mediators in normal and osteoarthritic sow chondrocytes. *J Med Food*. 2005;8:149–153.
22. Rahman L, Lembang RS, Lallo S, Handayani SR, Permana AD. Bioadhesive dermal patch as promising approach for improved antibacterial activity of bioactive compound of *Zingiber cassumunar* Roxb in ex vivo *Staphylococcus aureus* skin infection model. *Drug Deliv Sci Technol*. 2021;63:102522.
23. Abdallah MH, Elghamry HA, Khalifa NE, et al. Ginger extract-loaded sesame oil-based niosomal emulgel: quality by design to ameliorate anti-inflammatory activity. *Gels*. 2022;8:737.
24. Danciu C, Vlaia L, Fetea F, et al. Evaluation of phenolic profile, antioxidant and anticancer potential of two main representatives of Zingiberaceae family against B16A5 murine melanoma cells. *Biol Res*. 2015;48:1–9.
25. Sharif MF, Bennett MT. The effect of different methods and solvents on the extraction of polyphenols in ginger (*Zingiber officinale*). *Jurnal Teknologi*. 2016;78:11.
26. Costanzo M, Esposito E, Guizzato M, et al. Formulative study and intracellular fate evaluation of ethosomes and transethosomes for vitamin D3 delivery. *Int J Mol Sci*. 2021;22:5341.
27. Khan DH, Bashir S, Khan MI, Figueiredo P, Santos HA, Peltonen L. Formulation optimization and in vitro characterization of rifampicin and ceftriaxone dual drug loaded niosomes with high energy probe sonication technique. *Drug Deliv Sci Technol*. 2020;58:101763.
28. Ahmad AM, Mohammed HA, Faris TM, et al. Nano-Structured lipid carrier-based oral glutathione formulation mediates renoprotection against cyclophosphamide-induced nephrotoxicity, and improves oral bioavailability of glutathione confirmed through RP-HPLC micellar liquid chromatography. *Molecules*. 2021;26:7491.
29. Aboubakr EM, Mohammed HA, Hassan AS, Mohamed HB, El Dosoky MI, Ahmad AM. Glutathione-loaded non-ionic surfactant niosomes: a new approach to improve oral bioavailability and hepatoprotective efficacy of glutathione. *Nanotech Rev*. 2022;11:117–137.
30. D'Souza R, Mutalik S, Venkatesh M, Vidyasagar S, Udupa N. Nasal insulin gel as an alternate to parenteral insulin: formulation, preclinical, and clinical studies. *AAPS PharmSciTech*. 2005;6:E184–E189.

31. Gao S, Tian B, Han J, et al. Enhanced transdermal delivery of lornoxicam by nanostructured lipid carrier gels modified with polyarginine peptide for treatment of carrageenan-induced rat paw edema. *Int J Nanomedicine*. 2019;14:6135–6150.
32. Aiyalu R, Govindarajan A, Ramasamy A. Formulation and evaluation of topical herbal gel for the treatment of arthritis in animal model. *Braz J Pharm Sci*. 2016;52:493–507.
33. Aref ZF, Bazeed S, Hassan MH, et al. Possible role of ivermectin mucoadhesive nanosuspension nasal spray in recovery of post-COVID-19 anosmia. *Infect Drug Resist*. 2022;15:5483–5494.
34. Faisal W, Soliman GM, Hamdan AM. Enhanced skin deposition and delivery of voriconazole using ethosomal preparations. *J Liposome Res*. 2018;28:14–21.
35. Alhakamy NA, Kotta S, Ali J, et al. Formulation development, statistical optimization, in vitro and in vivo evaluation of etoricoxib-loaded eucalyptus oil-based nanoemulgel for topical delivery. *Appl Sci*. 2021;11:7294.
36. Soliman SM, Malak NA, El-Gazayerly ON, Rehim AA. Formulation of microemulsion gel systems for transdermal delivery of celecoxib: in vitro permeation, anti-inflammatory activity and skin irritation tests. *Drug Discov Ther*. 2010;4:459–471.
37. Kaur K, Jain S, Sapra B, Tiwary AK. Niosomal gel for site-specific sustained delivery of anti-arthritis drug: in vitro-in vivo evaluation. *Current Drug Delivery*. 2007;4:276–282.
38. Escibano E, Calpena AC, Queral J, Obach R, Doménech J. Assessment of diclofenac permeation with different formulations: anti-inflammatory study of a selected formula. *Eur J Pharm Sci*. 2003;19:203–210.
39. Elsewedy HS, Younis NS, Shehata TM, Mohamed ME, Soliman WE. Enhancement of anti-inflammatory activity of optimized niosomal colchicine loaded into jojoba oil-based emulgel using response surface methodology. *Gels*. 2021;8:16.
40. Hofni A, El-Moselhy MA, Taye A, Khalifa MM. Combination therapy with spironolactone and candesartan protects against streptozotocin-induced diabetic nephropathy in rats. *Eur J Pharmacol*. 2014;744:173–182.
41. Eltobshi AA, Mohamed EA, Abdelghani GM, Nouh AT. Self-nanoemulsifying drug-delivery systems for potentiated anti-inflammatory activity of diacerein. *Int J Nanomedicine*. 2018;13:6585–6602.
42. Abdulbaqi IM, Darwis Y, Abou Assi R, Khan NAK. Transethosomal gels as carriers for the transdermal delivery of colchicine: statistical optimization, characterization, and ex vivo evaluation. *Drug Des Devel Ther*. 2018;12:795.
43. Duangjit S, Opanasopit P, Rojanarata T, Ngawhirunpat T. Characterization and in vitro skin permeation of meloxicam-loaded liposomes versus transfersomes. *J Drug Deliv*. 2011;2011:418316.
44. Jain S, Jain P, Umamaheshwari R, Jain N. Transfersomes—a novel vesicular carrier for enhanced transdermal delivery: development, characterization, and performance evaluation. *Drug Dev Ind Pharm*. 2003;29:1013–1026.
45. Gaumet M, Vargas A, Gurny R, Delie F. Nanoparticles for drug delivery: the need for precision in reporting particle size parameters. *Eur J Pharm Biopharm*. 2008;69:1–9.
46. Abdellatif AAH, Rasheed Z, Alhowail AH, et al. Silver citrate nanoparticles inhibit PMA-induced TNF $\alpha$  expression via deactivation of NF- $\kappa$ B activity in human cancer cell-lines, MCF-7. *Int J Nanomedicine*. 2020;15:8479–8493.
47. Hussein UK, Hassan NE, Elhalwagy ME, et al. Ginger and propolis exert neuroprotective effects against monosodium glutamate-induced neurotoxicity in rats. *Molecules*. 2017;22:1928.
48. Maheswari P, Ponnusamy S, Harish S, Ganesh M, Hayakawa Y. Hydrothermal synthesis of pure and bio modified TiO<sub>2</sub>: characterization, evaluation of antibacterial activity against gram positive and gram negative bacteria and anticancer activity against KB Oral cancer cell line. *Arab J Chem*. 2020;13:3484–3497.
49. Karthickeyan V. Effect of nature based antioxidant from Zingiber officinale Rosc. on the oxidation stability, engine performance and emission characteristics with neem oil methyl ester. *Heat Mass Transfer*. 2018;54:3409–3420.
50. Begum MY, Abbulu K, Sudhakar M. Preparation, characterization and in vitro release study of Flurbiprofen loaded stealth liposomes. *Chem Sci Trans*. 2012;1:201–209.
51. Verma P, Pathak K. Nanosized ethanolic vesicles loaded with econazole nitrate for the treatment of deep fungal infections through topical gel formulation. *Nanomedicine*. 2012;8:489–496.
52. Salem HF, Nafady MM, Kharshoum RM. Novel enhanced therapeutic efficacy of dapoxetine HCl by nano-vesicle transdermal gel for treatment of carrageenan-induced rat paw edema. *AAPS Pharm Sci Tech*. 2020;21:1–13.
53. Ali MFM, Salem HF, Abdelmohsen HF, Attia SK. Preparation and clinical evaluation of nano-transfersomes for treatment of erectile dysfunction. *Drug Des Devel Ther*. 2015;9:2431.
54. Khurana S, Jain N, Bedi P. Nanoemulsion based gel for transdermal delivery of meloxicam: physico-chemical, mechanistic investigation. *Life Sci*. 2013;92:383–392.
55. El-Badry M, Fetih G, Fathalla D, Shakeel F. Transdermal delivery of meloxicam using niosomal hydrogels: in vitro and pharmacodynamic evaluation. *Pharm Dev Technol*. 2015;20:820–826.
56. Tawfeek HM, Abdellatif AA, Abdel-Aleem JA, Hassan YA, Fathalla D. Transfersomal gel nanocarriers for enhancement the permeation of lornoxicam. *Drug Deliv Sci Technol*. 2020;56:101540.
57. Kapadia R, Khambete H, Katara R, Ramteke S. A novel approach for ocular delivery of Acyclovir via niosomes entrapped in situ hydrogel system. *J Pharm Res*. 2009;2:745–751.
58. El-Sonbaty MM, Akl MA, Khalid M, Kassem AA. Does the technical methodology influence the quality attributes and the potential of skin permeation of Luliconazole loaded transethosomes? *Drug Deliv Sci Technol*. 2022;68:103096.
59. Kaur M, Singh K, Jain SK. Luliconazole vesicular based gel formulations for its enhanced topical delivery. *J Liposome Res*. 2020;30:388–406.
60. Verma D, Fahr A. Synergistic penetration enhancement effect of ethanol and phospholipids on the topical delivery of cyclosporin A. *J Control Release*. 2004;97:55–66.
61. Ghanbarzadeh S, Arami S. Enhanced transdermal delivery of diclofenac sodium via conventional liposomes, ethosomes, and transfersomes. *Biomed Res Int*. 2013;2013:616810.
62. Rujirek C, Siriwan O, Siriwan T, Prachya K, Ampai P, Vichai R. Chondroprotective potential of bioactive compounds of Zingiber cassumunar Roxb. against cytokine-induced cartilage degradation in explant culture. *J Med Plant Res*. 2012;6:5204–5213.
63. Han A-R, Kim H, Piao D, Jung C-H, Seo EK. Phytochemicals and bioactivities of Zingiber cassumunar Roxb. *Molecules*. 2021;26:2377.

**International Journal of Nanomedicine****Dovepress****Publish your work in this journal**

The International Journal of Nanomedicine is an international, peer-reviewed journal focusing on the application of nanotechnology in diagnostics, therapeutics, and drug delivery systems throughout the biomedical field. This journal is indexed on PubMed Central, MedLine, CAS, SciSearch®, Current Contents®/Clinical Medicine, Journal Citation Reports/Science Edition, EMBase, Scopus and the Elsevier Bibliographic databases. The manuscript management system is completely online and includes a very quick and fair peer-review system, which is all easy to use. Visit <http://www.dovepress.com/testimonials.php> to read real quotes from published authors.

Submit your manuscript here: <https://www.dovepress.com/international-journal-of-nanomedicine-journal>